Title

Interferon Regulatory Factor 4 amplifies Th2 responses through inhibition of Il31 expression

Author

Munoz Sandoval, Priscila

Publication Date

2024

Interferon Regulatory Factor 4 amplifies Th2 responses through inhibition of Il31 expression

by
Priscila Munoz Sandoval

DISSERTATION
Submitted in partial satisfaction of the requirements for degree of
DOCTOR OF PHILOSOPHY

in

Biomedical Sciences

in the

GRADUATE DIVISION
of the
UNIVERSITY OF CALIFORNIA, SAN FRANCISCO

Approved:

DocuSigned by:
Dean Sheppard
101CEA27F0AF442...

Dean Sheppard
Chair

DocuSigned by:
Tiffany Scharschmidt
DocuSigned by:
K. Mark Ansel
BC645044B450408...

Tiffany Scharschmidt

K. Mark Ansel

Committee Members

DEDICATION

Para mis abuelitos, su amor y apoyo incondicional no tiene fronteras. A mis padres que dejaron todo y me enseñaron como luchar. Para mi mamá, Carmen que siempre cree en mi y para mi hermano, Tona.

ACKNOWLEDGEMENTS

The last six years would not be possible were in not for the incredible support of my mentors and encouragement of from my loved ones.

To my mentor Mark Ansel, thank you for all your understanding, support, and encouragement during my graduate career. When life kept throwing me curveball after curveball you gave me the grace that I needed in order to make sure I took care of my health. You are an incredible scientist who lets his trainees be creative with their science and encourage scientific curiosity. I have always admired that your commitment to justice, diversity, and inclusion. Thank you for supporting all my endeavors, from the formation of ImmunoDiverse to mentoring a PROPEL scholar, I felt mentored in a holistic manner, and I will forever be grateful that I could bring my full self to lab.

To my thesis committee, Dean Sheppard, and Tiffany Scharschmidt. Thank you for your scientific insight and encouragement, this body of work was made better because of your input. I would also like to thank Dr. Ari Molofsky, who formed part of my qualifying exam committee.

This thesis would not exist were it not for the seminal work Dr. Marlys Fassett has done in the Ansel lab and now in her own lab. I rotated in Mark's lab because I fell in love with the IL-31 project and am thankful to have had your mentorship in getting this project to where it is today.

I'd also like to thank the BMS program coordinators and staff for all for all their help throughout the years making navigating rotations, qualifying exams, dissertation process go as smoothly as possibly (Meredith Miner, Demain Sainz, Ned Molyneaux, Marcelo Pereira, Priscila Pereira, Amanda Andodian). I would like to extend a special thank you

Manlio Maineri for his administrative help in the Ansel Lab, especially in getting orders in to perform last minute experiments.

I am grateful to have been part of a lab with helpful individuals that valued collaboration. Thank you to our lab managers and research assistants Darryl Mar, Simon Zhou, Simon Wong, Suparna Roy, Jaela Caston, and Celeste Garza. To Celeste, especially, you are an incredible scientist, hardworking, passionate, and I am incredibly grateful for being given the chance to be your mentor and to see how much you grew as a scientist in the lab. This project was made better because of you, and I thank you for the long hours of troubleshooting and the many CRISPR experiments. Having a fellow Latina in the lab made my graduate career all that much more rewarding. To the other grad students in the lab Did Zhu and Benjamin Wheeler I am so fortunate to have overlapped with the two of you. Didi, you are such a thoughtful and rigorous scientist. Thank you for making me a better scientist and your friendship. I am so lucky to have you and Kamir Hiam to share food adventures with.

To Oscar Aguilar Alfaro, you are such a kind human and so incredibly hardworking, thank you for always making space for others and paving the way to other Latine scientists. You make science accessible and fun.

I would not be the scientist I am today without my experience in the Rosenblum lab. To Mike Rosenblum, I came to your lab with the goal of going to grad school and was able to accomplish exactly that through your mentorship. I grew so much as a scientist during my time in your lab. Thank you for trusting me to lead human projects and to have my own mouse project and for always reminding me to think of the big picture, place experiments into context before delving into the data. You created an lab environment

that was incredibly fun but also executed excellent scientist. Thank you to my mentors during my time in the Rosenblum Lab, Maggie and Mariela. The two of you are incredible scientists and role models.

Grad school was incredibly difficult with many ups and downs, but I made beautiful friendships that helped me get through the tough times and celebrate the good times.

Nour Abdulhay, Yewande Alibi, Jocelyn Lopez, Carlos Suazo, Harold Marin, Megan Montoya, Evelyn Hernandez, Bahar Zirak you have all been there to vent about the difficult times and to share in happy moments. To Evelyn Hernandez, you are an incredible mujer, thank you me feel like I am home when we cook our comida Mexicana. To Celeste Linhares, I couldn't have asked for a better roommate and friend. Thank you for the baked goods, ice cream and for being there for some of my toughest moments. To Bahar Zirak, I have known you for as long as I have lived in the bay, and I treasure our friendship so much. From being transfer students at UC Berkeley, to serendipitously crossing paths in the Rosenblum lab, starting, and finishing grad school together. I couldn't have asked for a kinder and truer friend to have shared all the challenges, tears, joy, and laughter of the last six years. Lokesh Kalekar, all good things, always. You are an amazing scientist and if even possible an even more amazing friend.

Thank you to my R.I.S.E family, Putri Ramaputri, Paola Mora, Madeleine Villanueva, Angelica Vargas, Aureo Mesquita. We all met at UC Berkeley and our friendship has only continued to grow. The pandemic was incredibly difficult, but I looked forward to every Tuesday night for our Zoom calls where we would catch up, play games, and laugh so much. Putri, Paola, Madeleine, Angelica aka Levi and Ruben's tias thank you for lifting me up during my darkest moments and for celebrating all my wins. You all understand me

in a way many people don't, you make my life better, you make me a better human. I love you all dearly.

Thank you to Arlene Luna, Caitlin Biljan, and Laura Drennen, you ladies inspire me every day with your kindness, strength, and drive. You've all shown me what it means to trust oneself after difficult times and to come out on the other end better, happier, stronger. I am so grateful Arlene brought us all together.

To Julian Delgado (and Lalo) thank you for loving and accepting all of who I am. You give me so much strength and often believe in me more than I believe in myself. I can't wait to make many more memories with you.

A toda mi familia, thank you for all your encouragement, love, and support. Mis abuelitos that are no longer here, Ramiro y Lidia, thank you for being my first parents, for pouring so much into me and especially mi abuelita for always telling me to go after what I want. Los extraño y quiero tanto. Thank you to my brother Tonatiuh (Tona) for always making it a point to visit me, for making me laugh so much, for sharing the tastiest meals, and for all of your support. Your visits are one of the highlights of my year. I am incredibly proud to be your sister. To mi mamá, there are not enough words to tell you how much you mean to me. You've always believed in me, and I am the mujer I am today because of your encouraging words and love, gracias.

CONTRIBUTIONS

Chapters 2 and 3 are part of a manuscript in preparation. The following authors contributed to the project: Celeste Garza, Marlys Fassett, K Mark Ansel. Marlys and Mark helped with experimental design, data interpretation and manuscript writing.

IRF4 AMPLIFIES TH2 RESPONSES THROUGH INHIBITION OF IL31 EXPRESSION

Priscila Muñoz Sandoval

ABSTRACT

Th2 cells are specialized to control helminths and other parasites. The protective response induced by Th2 cells, known as the type 2 immune response, is driven by their secretion of the canonical cytokines IL-4, IL-5, and IL-13. IL-31 is a lesser known Th2 cytokine that limits the magnitude of type 2 inflammation in the skin. However, little is known about how IL-31 regulates immune responses in other tissues such as the lung and gut. Here we examined how *Il31* deficiency alters lung and gut immune responses to the helminth *Nippostrongylus brasiliensis* (*N.b.)*, a model of type 2 immunity. Compared to wildtype controls, *Il31*-deficient mice infected with *N.b.* had accelerated worm clearance and increased GATA3 and IL-13 expressing Th2 cells in the intestine. CD4+ T cells were the predominant producers of IL-31 in the lung and intestine, as identified by a newly generated *Il31* reporter mouse. To identify pathways that control *Il31* transcription in mouse Th2 cells, we conducted a pooled loss-of-function CRISPR screen. This screen identified the calcium sensor *Stim1* as an *Il31* activator, and *Irf4,* a transcription factor that positively regulates IL-4 and IL-13 production, as an *Il31* repressor. *Irf4* deletion increased IL-31 production in both mouse and human primary Th2 cells. In vivo, selective deletion of *Irf4* only in *Il31* expressing cells increased intestinal *N.b.* worm burden, indicating that *Irf4* supports type 2 responses by limiting IL-31 and positively regulating canonical type 2 cytokines in IL-31-producing helper T cells.

TABLE OF CONTENTS

TABLE OF FIGURES

Chapter 2

Chapter 3

Chapter 4

LIST OF TABLES

Chapter 3

CHAPTER 1: GENERAL INTRODUCTION

T cells

T cells are involved in the adaptive immune response and are responsible for mediating immune responses against pathogens and various types of diseases. Development of T cells begins in the thymus from bone marrow (BM) derived thymocyte. They undergo a complex maturation process in the thymus where they go through a series of developmental stages. These include a selection process that includes cells that go through double negative (CD4-CD8-, DN), double positive (CD4+CD8+), and finally single positive (CD4+CD8- or CD4-CD8+) states (Germain, 2002). This process involves rigorous selection to ensure the generation of a diverse T cell repertoire capable of recognizing a vast array of antigens. Mature T cells migrate to peripheral lymphoid tissues, where they encounter antigen presented by antigen-presenting cells (APCs). Antigen recognition triggers T cell activation, leading to clonal expansion and differentiation into effector and memory T cell subsets. These subsets include cytotoxic CD8+ T cells which directly target and kill cells via their secretion of effector molecules. CD4+ T cells help in the protection from pathogens but can also modulate and regulate an immune response to prevent aberrant and prolonged inflammation. CD4+ T cells aid in the immune response via their production of cytokines and chemokines.

Th2 cells

Th2 cells are a critical subset of CD4 + T helper cells that play a pivotal role in the type 2 immune response. These cells are primarily involved in the defense against extracellular pathogens such as helminths but when dysregulated can contribute to chronic inflammatory diseases such as asthma and allergy. Th2 cells are characterized by their

production of a distinct cytokine profile that includes IL-4, IL-5, and IL-13(Walker & McKenzie, 2017). These secreted cytokines have pleiotropic effects on various immune and non-immune cells. IL-4 is a key factor in activation of B-cell proliferation, promotes immunoglobulin (Ig) class switching and antibody production. IL-4 and IL-13 also facilitate the recruitment and activation of eosinophils and basophils, alternative macrophage activation and mast cell degranulation. By promoting B cell class switching to IgE, activating eosinophils, and inducing mucus production, Th2 cells contribute to the elimination of extracellular parasites. However, an imbalanced Th2 response can lead to the development of allergic diseases, such as asthma and atopic dermatitis, due to excessive inflammation and tissue remodeling.

Cytokines

Cytokines play a crucial role in maintaining immune homeostasis and host defense against pathogens. They are a diverse group of soluble proteins or glycoproteins that regulate the intensity and duration of an immune response and are produced by a variety of cells, including immune cells. Cytokines act in a complex and interconnected manner, forming intricate networks that regulate various immune functions. They can act in an autocrine, paracrine, or endocrine manner, influencing the behavior of the producing cell, neighboring cells, or distant target cells, respectively. Cytokine signaling pathways involve receptor-mediated activation of intracellular signaling cascades, leading to changes in gene expression and cellular responses. Cytokines play a crucial role in maintaining immune homeostasis and host defense against pathogens. However, dysregulation of cytokine production or signaling can contribute to the pathogenesis of various diseases, including autoimmune diseases, inflammatory disorders, allergies, and cancer.

IL-31

Interleukin 31 (IL-31) is a cytokine mainly secreted by Th2 CD4+ T cells (Dillon et al., 2004). It is part of the IL-6 pro-inflammatory family of cytokines but unlike other members of this family, IL-31 signals via its heterodimeric receptor IL31RA/OSMRβ whereas other IL-6 family cytokines signal through a heterodimeric complex that includes gp130 (Bilsborough et al., 2010). Studies carried out in mouse models as well as clinical data from patients with atopic dermatitis (AD) suggest that IL-31 is involved in the pathogenesis of itchy inflammatory skin diseases (Mollanazar et al., 2016). IL-31 may have distinct roles in different contexts of the immune response due to the expression of its receptor, IL-31RA in various tissues and the functional diversity of IL-6 family members.

CHAPTER 2: ANALYSIS OF THE ROLE OF IL-31 IN TYPE 2 IMMUNE RESPONSES IN THE LUNG AND SMALL INTESTINE

Introduction

Many studies have focused on what happens to the immune response in the presence or absence of IL-31 receptor, IL-31RA encoded by *Il31ra*. IL-31RA expression is increased in both lung tissue and lung cellular infiltrates in a mouse model of airway hyper-responsiveness (Dillon et al., 2004). Studies carried out on IL-31RA deficient mice showed that IL-31 negatively regulated Th2 cytokine-dependent immunity and inflammation. After intravenous injection of *Schistosoma mansoni* eggs, *Il31ra*$^{-/-}$ mice developed exacerbated pulmonary granulomatous inflammation and had higher levels of IL-4, IL-5, and IL-13 in draining lymph nodes compared to wild-type controls (Perrigoue et al., 2007). In a follow-up study the IL-31RA deficient mice exhibited enhanced intestinal inflammation and Th2 cytokine responses following Trichuris infection (Perrigoue et al., 2009). These observations are contrary to the theory that IL-31 plays an active role in promoting the development and exacerbation of Th2-associated disease.

In contrast, it has been reported that IL-31RA deficient mice exhibited increased responsiveness to OSM (oncostatin M) and enhanced production of OSM-inducible cytokines, such as IL-5 and VEGF, during airway sensitization and challenge, suggesting that susceptibility of IL-31RA deficient mice to exacerbated Th2-type disease is an indirect result of IL-31RA deletion that leads to an elevated responsiveness to OSM (Bilsborough et al., 2010). A possible explanation for these seemingly contradictory roles of IL-31 might depend on tissue specific cell types expressing IL-31 RA. For example, IL-31 receptor signaling positively regulates Th2 responses induced by nasal administration of the

Japanese cedar polled allergen, but negatively regulates these responses following intraperitoneal injection (Saito et al., 2017). Alternatively, we recently demonstrated the crosstalk of immune cells and neurons where IL-31 expression indirectly affects IL-4 expression via the CGRP receptor in neurons.

IL-31 receptor blockade by a humanized anti-human IL-31RA monoclonal antibody, Nemolizumab, effectively alleviates itch in patients with atopic dermatitis and prurigo nodularis, and improves skin lesions in most patients (Kabashima et al., 2018, 2020; Kwatra et al., 2023; Silverberg et al., 2020; Ständer et al., 2020). However, adverse effects included unexpected asthma and dermatitis flares in a subset of patients, and increased serum concentration of the IL4RA-responsive chemokine TARC (CCL17). CCL17, which has been used as the most reliable biomarker for AD, was elevated in bronchoalveolar fluid of patients with asthma, and associated with the development of murine colitis. Not only did some patients exhibit cytokine abnormalities but patients with a history of asthma had a greater incidence of asthma events in a dose dependent fashion. Some patients also had in increased incidence of gastroenteritis, (Kabashima et al., 2020; Lupancu et al., 2023; Mihara et al., 2019; Silverberg et al., 2020). The clinical sequalae that have emerged as side effects of nemolizumab treatment suggest the importance of understanding what inputs regulate IL-31 expression in different contexts and how the immune response is affected not only in the skin but importantly in the lung and intestine as well.

Results

IL-31 Deficiency Results In Accelerated Type 2 Immune Response

To identify cells that produce IL-31 and determine how IL-31 modulates type 2 immune responses in tissues other than skin, we generated *Il31* transcriptional reporter mice designated Red31 (R31), recombinase expression detector for IL-31 (**Fig. 2.1A**). Cells from these mice contain a knock-in transgene that includes a tandem dimer red fluorescent protein (tdTomato) linked by an internal ribosomal entry site (IRES) to a Cre element. This transgene replaces the translation initiation site of the endogenous *Il31* gene thus marking cells that would produce IL-31 with tdTomato, while the Cre element allows for conditional deletion studies in IL-31 producing cells. Red31 homozygous mice $Il31^{R31/R31}$ (R31/R31) are rendered *Il31*-deficient. To validate that the *Red31* transgene disrupts the endogenous *Il31* gene and that Red31 tdTomato fluorescence correlates with IL-31 production, we sorted Th2 polarized cells from R31/wt mice and assessed Il31 reads from bulk sequencing data (**Fig. 2.1B**)

To uncover consequences of *Il31* deficiency for allergic inflammation and to determine how *Il31* deficiency alters IL-13-producing type 2 immune cells in particular, we crossed *Red31* transgenic mice with *Il13* reporter strain $Il13^{Smart/Smart}$(Smart13) (Liang et al., 2011). Combining the *Red31* (R31) and *Smart13* (Sm13) transgenes allows identification of live cells that transcribe *Il31* and/or *Il13*. In addition, the *Red31* transgene interrupts endogenous *Il31* gene production, so homozygous *Red31* transgenic mice (R31.R31) are *Il31* deficient. Therefore, in experiments performed on R31/R31.Sm13 transgenic mice, we can simultaneously assess consequences of *Il31* deficiency and detect individual cells

that express *Red31*, *Sm13*, or both. In this experimental context, we can measure how *Il31* deficiency impacts *Il13* production and alterations in *Il13*-producing cells.

We challenged *Il31*$^{R31/R31}$.*Il13*$^{Sm/+}$(R31/R31.Sm13$^{+/wt}$) mice with 500 larvae of the parasitic helminth *Nippostrongylus brasiliensis* (*N.b*) to assess systemic mucosal infection in the absence of IL-31 (**Fig.2.1C**). Intestinal worm burden differed at day 5 post infection, at which time R31/R31.Sm13$^{+/wt}$ mice had mostly cleared intestinal worms (<40), while control mice (Sm13$^{+/wt}$) had ~125 remaining worms (**Fig. 2.1C**). By day 7 post infection both R31/R31.Sm13$^{+/wt}$ mice and control mice had cleared intestinal worms (**Fig. 2.1D**).

We assessed inflammation in the lung and gut by flow cytometry and histology at day 5 post-infection. In the lung *N.b.* infection induced equally robust proportions of Th2 cells expressing the master regulator transcription factor GATA3 and the IL-13 reporter in R31/R31.Sm13/wt and control mice (**Supp Fig. 2.1A-G**). IL-4 and IL-13 production was also similar in lung cells restimulated ex vivo for intracellular cytokine staining (**Supp Fig. 2.1H-K**). However, the proportion of small intestinal lamina propria (siLP) CD4+ T cells expressing GATA3 was 2-fold greater in R31/R31.Sm13/wt mice compared to control Sm13$^{+/-}$ (**Fig.2.1 E-G**). But the proportion of RORgt+ CD4+ T cells did not change (**Fig.2.1 E-G**). Additionally, R31/R31Sm13$^{+/-}$ CD4 T cells had increased proportions of IL-13 reporter expressing cells (**Fig.2.1 H,I**) with no differences in the overall proportion of CD45+ and CD4+ T cells (**Fig. 2.1J,K**). We assessed mucus production at day 5 post infection in the small intestine by PAS staining. More mucus production was detectable in R31/R31.Sm13/wt intestinal tissue sections (**Fig.2.1L**). These data demonstrate that IL-31 attenuates the type 2 immune response to *N.b.* infection in the gut and suggest that

increased type 2 intestinal inflammation accelerates worm clearance in *Il31*-deficient mice versus control mice.

CD4 T cells Are The Predominant Source Of IL-31 In The Lung After Helminth Infection

To identify all cell types that express *IL31* during *N.b.* infection, we generated a lineage-tracing mouse strain that enables visualization of cells that have ever expressed *Il31 in vivo*. To generate this strain, termed 'R31.Ai14', we crossed R31/R31 mice with mice bearing the Cre-activated tdTomato reporter transgene Ai14 (Gt(ROSA)26Sor$^{tm14(CAG-tdTomato)Hze}$ (Madisen et al., 2009). All cells in the heterozygous R31.Ai14 mice bear one copy each of R31 and Ai14 transgenes. In these animals, Red31 transgene expression induces cell-intrinsic Cre-mediated genomic rearrangement to activate the Ai14 transgene, which can be visualized as bright stable tdTomato fluorescence. As a result, tdTomato fluorescence highlights cells that have ever transcribed *Red31* as well as their progeny. We confirmed the fidelity of tdTomato fluorescence as an *Il31* reporter in Red31.Ai14(tdTomato) cells by measuring tdTomato fluorescence and IL-31 protein expression from the remaining *Il31* allele with a validated anti-mouse IL-31-specific mAb specific in fixed, permeabilized cells (**Fig. 2.1A**).

Next, we inoculated *R31.Ai14* mice with 500 *N.b* larvae via subcutaneous injection to identify cells that express Red31(*Il31)* as part of the inflammatory response to *Nb* infection. To do so, we harvested lung and small intestine on day 5 post infection to visualize *Il31*-expressing cells, which in R31.Ai14 mice are detectable by cell-intrinsic tdTomato expression. Immunofluorescence microscopy of lung tissue sections at this timepoint demonstrated many more R31.Ai14(tdTomato+) cells in *Nb*-infected mice verus

mock-infected R31.Ai14 control animals, indicating that *Nb* infection induces proliferation of pre-existing *Il31*-expressing cells, de novo expression of *Il31* in other cells, and/or recruitment of *Il31*-expressing cellss from other tissues (**Fig 2.2B**). Many of the R31.Ai14(tdTomato)+ cells in *Nb* infected lung sections co-expressed the pan-T cell marker CD3+ and were located near neurons in the peribronchial adventitia (**Fig 2.2F**, right panel).

Further characterization of R31.Ai14(tdTomato+) CD45+ cells in *Nb*-infected lung by FACS revealed that most tdTomato+ cells were CD90+ (lymphoid) cells. Most of these were CD3+ (T cells) (**Fig 2.2**, left panel, **Supp 2.3 A,B**) of the CD4+ lineage (**Fig 2.2**, right panel). However, this approach also exposed substantial R31.Ai14(tdTomato+) populations that were CD90+ but CD3-, *i.e.* lymphoid cells other than CD3+ T cells. Together, these data suggest that other lung lymphoid cell subsets such as B cells, NK cells, or innate lymphoid cells can express *Il31* during *Nb* infection. Subset analysis of the R31.Ai14(tdTomato+) CD3+ $CD4^{neg}$ T cells showed similar proportions of CD8+ and CD8- cells. The latter may include gdT cells, NK T cells, or MAIT cells.

We also performed immunofluorescence microscopy to reveal the localization of R31.Ai14(tdTomato+) cells in small intestine (duodenal) tissue sections at day 5 post infection. Small intestine tissue sections were stained for CD45, CD3, and RFP. Immunofluorescence images confirmed that the majority of R31.Ai14(tdTomato+) cells in the intestine are CD3+ T cells that are intraepithelial, in the lamina propia, or found in areas where other immune cell populations localize (**Fig 2.3C. Supp Fig. 2.4 A, B. Supp Fig 2.5 A,B**). In the small intestine on *Nb* infection day 5, CD4 T cells (gated

CD90+CD3+CD4+) comprised almost all of the CD45+ R31.Ai14(tdTomato+) cells. We detected a few R31.Ai14(tdTomato+) lymphoid non-T cells (CD90+CD3-) and a few CD90+CD3+CD4- cell *(i.e.* T cells other than CD4s) in *Nb*-infected small intestine, but these represented smaller proportions than in lung. Similarly, the proportion of CD45+CD90.2+CD3- (non-T) lymphocytes within the R31.Ai14(tdTomato+) gate was smaller in small intestine compared to lung (**Fig 2.2 A,B**).

Together, these imaging and flow cytometry data from R31.Ai14(tdTomato+) reporter transgenic mice indicated that CD4+ T cells comprise the majority of *Il31*-expressing cells induced during type 2 anti-helminth immune responses in both the lung and the small intestine and motivate further examination of *Il31* expression in CD4 T cells.

Discussion

IL-31 biology has long been associated with itching and type 2 inflammatory skin diseases (Cevikbas & Steinhoff, 2012; Dillon et al., 2004; Sonkoly et al., 2006), but emerging evidence for extracutaneous side effects of biologics that target the IL-31 signaling pathway underscore the equal biological relevance of IL-31 in lung and gut immune responses (Ruzicka et al., 2017; Silverberg et al., 2021; Sofen et al., 2023). However, unanswered questions remain regarding which specific cell types produce IL-31 *in vivo*, what factors positively or negatively regulate IL-31 production in these cells, and what the functional consequences of IL-31 production in organs other than skin may be.

To highlight individual cells that produce IL-31 in response to a type 2 inflammatory stimulus in both lung and gut, we took advantage of the life cycle of *Nippostrongylus*

brasiliensis (*Nb),* a parasitic nematode that burrows into skin before invading lung parenchyma, where it is coughed up and swallowed for eventual excretion through the gastrointestinal tract(Bouchery et al., 2017; Camberis et al., 2003). While *Nb* is not very inflammatory in skin, its presence triggers robust, well-characterized type 2 immune responses in both lung and gut (Harvie et al., 2010; Maizels & Gause, 2023; Seidl et al., 2011). We were able to definitively identify *Il31*-producing cells in *Nb*-infected lung and gut by measuring expression of *Red31*, a novel tdTomato fluorescent protein knock-in/knock-out *Il31* reporter transgene we generated for this purpose. In uninfected mice, *Red31*-expressing cells were rare. However, shortly after *Nb* infection we recorded substantial increases in *Red31(*tdTomato)-expressing cells in lung and in gut. These *Red31(*tdTomato)-expressing cells in *Nb*-infected mice were predominantly lymphoid cells, and mostly CD4 T cells, analogous to what we observed by intracellular monoclonal antibody staining for intracellular IL-31 protein production in a skin allergy model (Fassett et al., 2023). However, during *Nb* infection the relative proportion of Red31+ cells in the T cell verus n on-T cell lymphocyte compartment differed by organ. Specifically, we observed a sizeable population of Red31+ CD90+ CD3- cells in the gut, but even higher proportion of these in the lung, indicating that other non-T cell lymphoid cell types such as innate lymphoid cells, and B cells may be a biologically-meaningful source of IL-31 in this anatomical niche.

We also report evidence that endogenous IL-31 production negatively regulates type 2 cytokine production and *Nb* worm clearance. In *Red31* homozygous transgenic mice, which are *Il31*-deficient, we observed more IL-13-producing CD4 T cells and decreased small intestine worm counts, indicating more robust and/or efficient type 2 inflammatory

responses clear the parasites when *Il31* is not expressed. This finding is consistent with previous reports that mice deficient in one subunit of the heterodimeric IL-31 receptor, *Il31RA*, exhibit exacerbated type 2 inflammation in response to another intestinal parasite, *Trichuris trichiura* (Perrigoue et al., 2009). We hypothesize that *Il31*-dependent negative regulation of type 2 inflammation-dependent *Nb* worm clearance requires the same TRPV1+IL31RA+CGRP+ sensory neuron-dependent regulatory circuit we recently described in HDM dermatitis (Fassett et al., 2023). Further identifying the responding cell types in the lung and gut could lead to a better understanding of the of the differences in relative contribution of IL-31 to the immune response in the lung and gut.

Methods

IL-31 reporter mice

R31 IL-31 mice were generated using homologous gene targeting in C57BL/6 embryonic stem cells. The previously published plasmid pK0915-DT(Lexicon) containing Basop8 reporter (Lelievre et al., 2007) was modified to express tdTomato, such that the cassette now contained genomic sequence of the rabbit β-globin gene partial exon 203, the gene encoding tdTomato (Clontech), encyphalomyocarditis virus IRES, humanized Cre recombinase, bovine growth hormone poly(a), and a *lox*P-flanked neomycin resistance cassette. Homologous arms straddling the *Il31* translation initiation site were amplified from C57BL/6 genomic DNA using Phusion polymerase and cloned into the cassette. The construct was then linearized and transfected by electroporation into C57BL/6 embryionic stem cells. Cells were grown on irradiated feeders with aminoglycoside in the media. Neomycin-resistant clones were screened and positive clones were selected, tested, and

injected into blastocysts. Male and female R31/+ offspring were intercrossed to yield R31/R31 homozygotes.

Mice

Female and male age and sex matched mice were used between 8-15 weeks of age (4-6 weeks for in vitro T cell culture assays). Red31 reporter mice were crossed with IL-13 reporter Smart13 (B6.129S4(C)-*Il13*$^{tm2.1Lky}$/J) mice and were obtained or generated as described (Liang et al) to generate R31/R31.Sm13+/wt. mice. These mice were then crossed to B6 constitutive Cas9-expressing mice (Platt et al., 2014) to generate the R31/R31.Sm13+/wt.GFPCas9 mice used for the CRISPR screen. All mice were housed and bred in specific pathogen-free conditions in the Animal Barrier Facility at the University of California, San Francisco. Euthanasia procedures and experimental protocols were approved by the Institutional Animal Care and Use Committee (IACUC) of the University of California, San Francisco.

Nippostrongylus brasiliensis infection

Mice were infected with 500 *N. brasiliensis* third stage larvae (L3) and were euthanized at the indicated timepoints for analysis of the mediastinal and mesenteric lymph nodes, lungs, and small intestine.

Tissue Processing

Whole lungs were minced and digested by gentle shaking in 5 mL of HBSS with 0.1 WU/mL Liberase TM (Roche) and 25μg.mL DNAse I (Roche) for 30 minutes at 37°C, and then mechanically dissocatied using GentleMACS C tubes (Miltenyi Biotec) followed by

a 70μM filter. Small intestinal lamina propria were processed as described (O'Leary et al., 2021).Lymph nodes were dissociated into single-cell suspension and passed through 70μM filter. Lungs were digested with 1.2mg/mL of Collagenase D (Roche) and 10U/mL of deoxyribonuclease I (Roche) for 30min at 37°C and dissociated with gentleMACS dissociator (Miltenyi Biotec). Enzymatic reaction was inhibited with cold PBS with 2% fetal bovine serum(FBS) (Omega). Cells were filtered through 70μM filter, pelleted through centrifugation and incubated with ACK Lysis Buffer (Gibco) to remove red blood cells before final suspension in PBS with 2% FBS.

Periodic Acid Schiff Stain

Lungs and small intestine were collected and fixed in formalin, paraffin embedded, sectioned, placed on glass slides, stained with Periodic Acid Schiff (PAS), digitally scanned on the Aperio AT2 scanner (Leica Biosystems, Inc) creating whole slide images (WSIs), and then uploaded to the HistoWiz cloud platform.

Histology

Mouse tissues were fixed in 10% formalin, embedded in paraffin, sectioned and stain with haematoxylin and eosin. The images were digitally scanned on the Aperio AT2 scanner (Leica Biosystems, Inc) creating whole slide images (WSIs), and then uploaded to the HistoWiz cloud platform.

Flow Cytometry

FC receptors of cells were blocked with anti-mouse CD16/32 (BioXCell). Cells were surface stained with anti-mouse monoclonal antibodies from BioLegend and BD

Biosciences including anti-CD4 (RM4-5), anti-CD8 (53-6.7), anti-CD45.1 (A20), anti-CD45.2 (104). Dead cells were excluded with Fixable Viability Dye eFluor780 (eBiosciences). Samples were collected with BD Fortessa and analyzed with FlowJo software (TreeStar). For intravascular staining, mice were anesthetized and injected with 2μg of anti-mouse CD45 (30-F11) in 100uL PBS by iv for ~3min and euthanized by CO_2 asphyxiation. For intracellular IRF4 expression, cells were fixed and permeabilized using Foxp3Transcription Factor Staining Buffer Set (eBiosciences).

Immunofluorescence

200um thick sections of proximal small intestine and lung were cut, washed in PBS and then blocked (24 hours 37°C, DPBS/0.3% TritonX-100/1% secondary-host serum/1% BSA). Samples were incubated in primary antibodies diluted in blocking solution (37°C, 48-72 hours), washed for 2 hours 3 times and incubated in secondary antibodies (37°C, 24 hours).

Imaging Antibodies

Primary antibodies used for murine imaging include rabbit anti-dsRed (Takara 632496, 1:400), goat anti-RFP (Rockland, 200-101-379, 1:400), rat anti-CD49f AF647 (Biolegend, 313610, 1:200), rat anti-CD49f AF488 (Biolegend, 313608, 1:200), rat anti-alpha Smooth Muscle Actin (Biotium, BNC040665, 1:100), rabbit anti-PGP9.5 (Abcam, ab108986, 1:200), rat anti-CD45 (Biolegend 103124 1:200), rat anti-CD3 (Biolegend 100209 1:200), rabbit anti-proSurfactant (Abcam, ab211326, 1:400). Secondary antibodies were used as necessary at protocol-specific concentrations, conjugated to A488, A555, AF594, and A647 (Life Technologies, Thermo-Fisher).

Confocal microscopy

Confocal images (for thick sections and T-cell quantification) were imaged using a Leica SP8 Upright laser-scanning confocal equipped with a 405nm laser and adjustable white light laser for excitation and imaging with 20x water immersion.

Image analysis

z-stacks were rendered in 3D and qualitatively analyzed using Bitplane Imaris v10.2 software package (Andor Technology PLC, Belfast, N. Ireland). Two slices per mouse and two animals per condition were analyzed. Representative images from each.

Figures

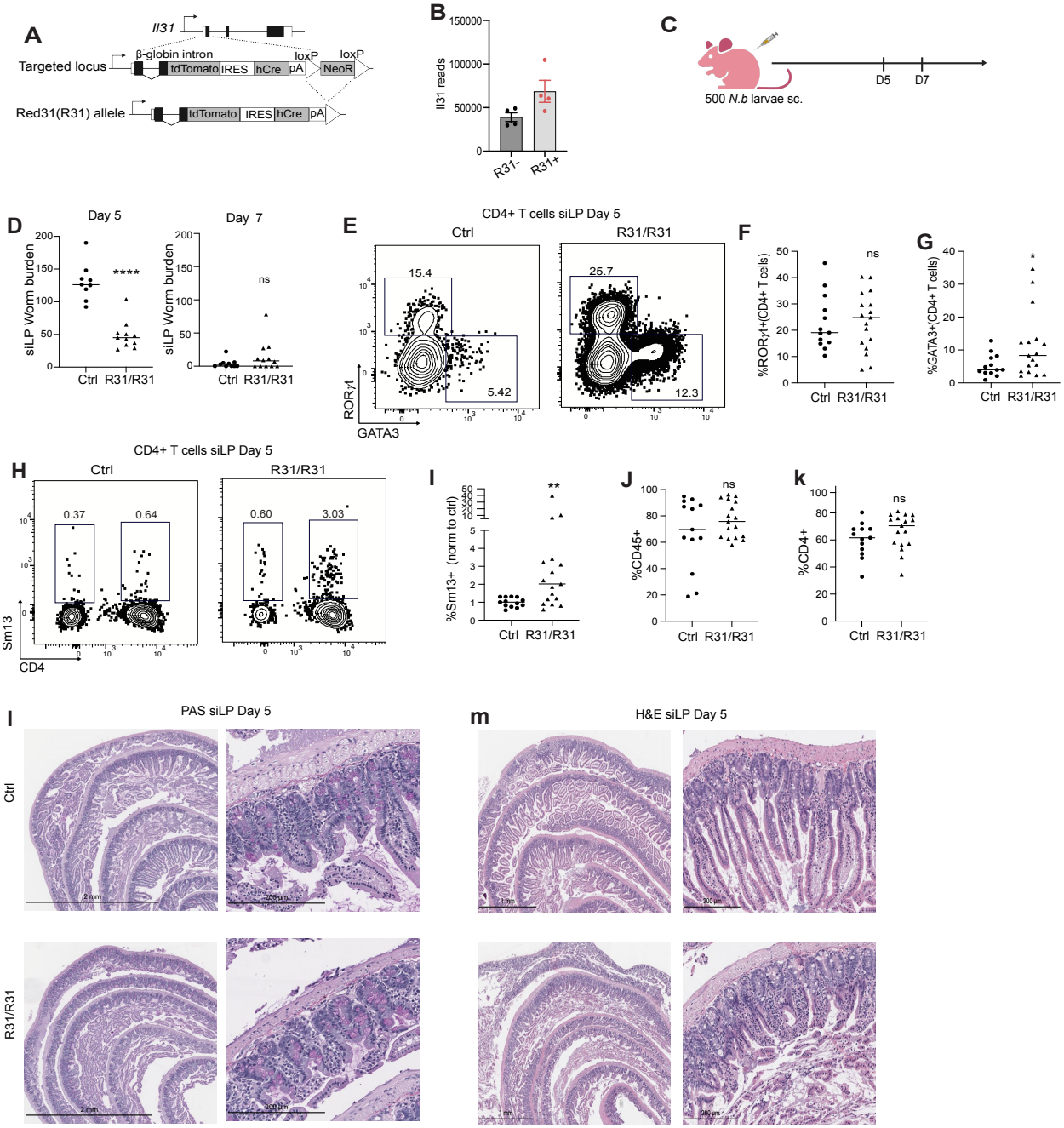

Figure 2.1 Accelerated worm expulsion and increased inflammation in the small intestine (a) Schematic or Red31 (R31) cassette (b) Il31 reads from bulk sequencing of in vitro differentiated Th2 cells. (c) Schematic of N.b infection model (d) Quantification of intestinal worm burden at day 5 and day 7 post infection. (e) Representative FACS plot showing RORgt and GATA3 expression of CD3+C4+ T cells from N.b infected mice on day 5 (f,g) Quantification of RORgt and GATA3 expression of CD3+C4+ T cells from N.b infected mice on day 5 (h) Representative FACS plot of Sm13+CD4+ T cells from small intestine of N.b infected mice on day 5 (i) Quantification of Sm13+ (IL-13 reporter) CD4+ T cells from small intesting of N.b infected mice on day 5 (j,k) Quantification of CD45+

and CD4+ cell populations in the small intestine at day 5 post N,b infection (l) Periodic-Acid Schiff staining of small intestine at day 5. (m) Representative image of H&E stain of the small intestine on day 5.

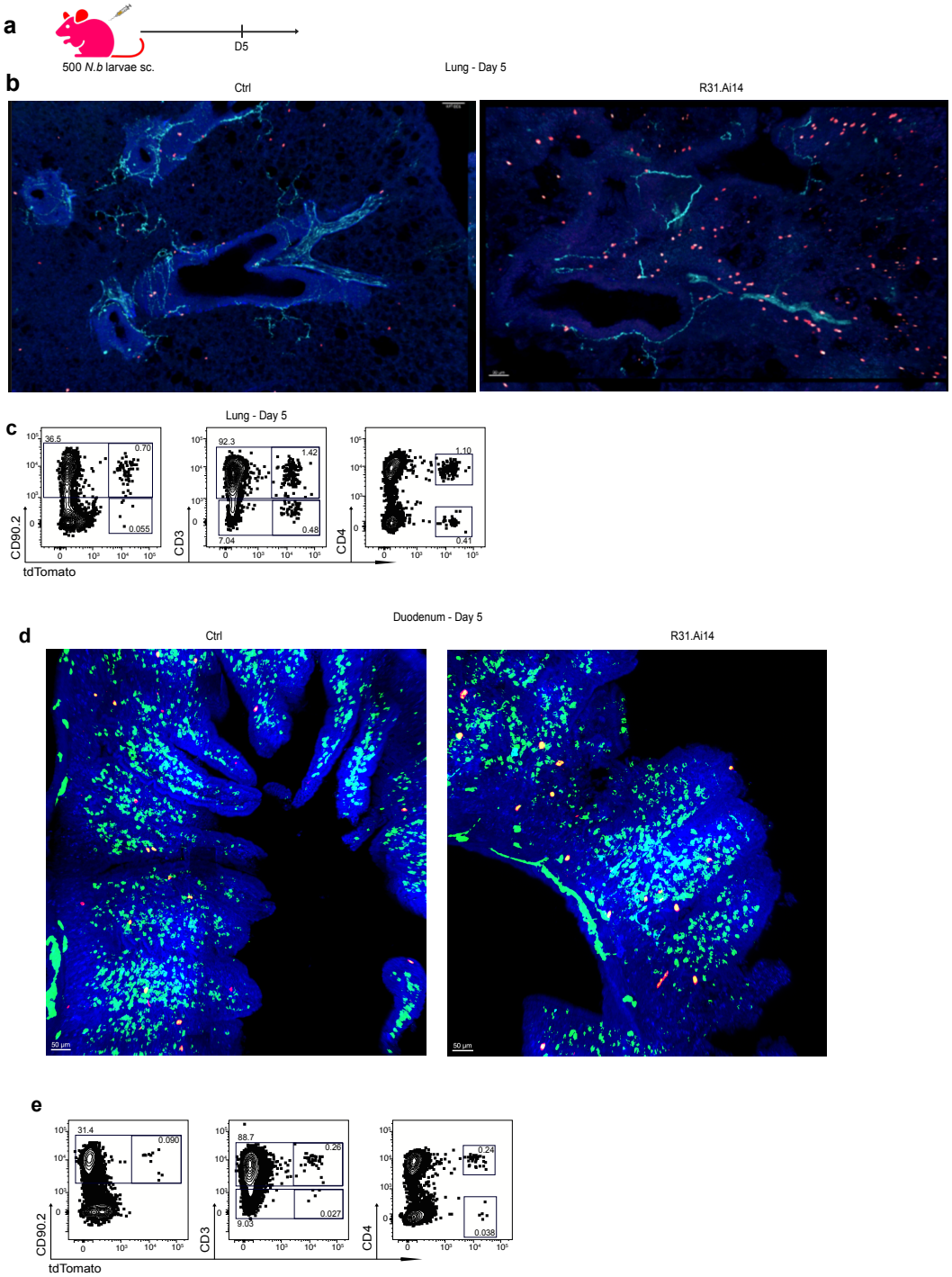

Figure 2.2 CD4+ T cells express IL-31 in the lung and intestine
(a) Schematic of N.b infection of Red31/wt.Ai14 mice (b)Immunofluorescent images of sham infected (left) and N.b infected (right) lung day 5 post infection (c) Representative FACS plot of frequency of CD90.2+, CD3+, and CD4+ populations expressing tdTomato at day 5 in the lung (d)Immunofluorescent images of sham infected (left) and N.b infected (right) small intestine at day 5 post infection (c) Representative FACS plot of frequency of CD90.2+, CD3+, and CD4+ populations expressing tdTomato at day 5 in the small intestine

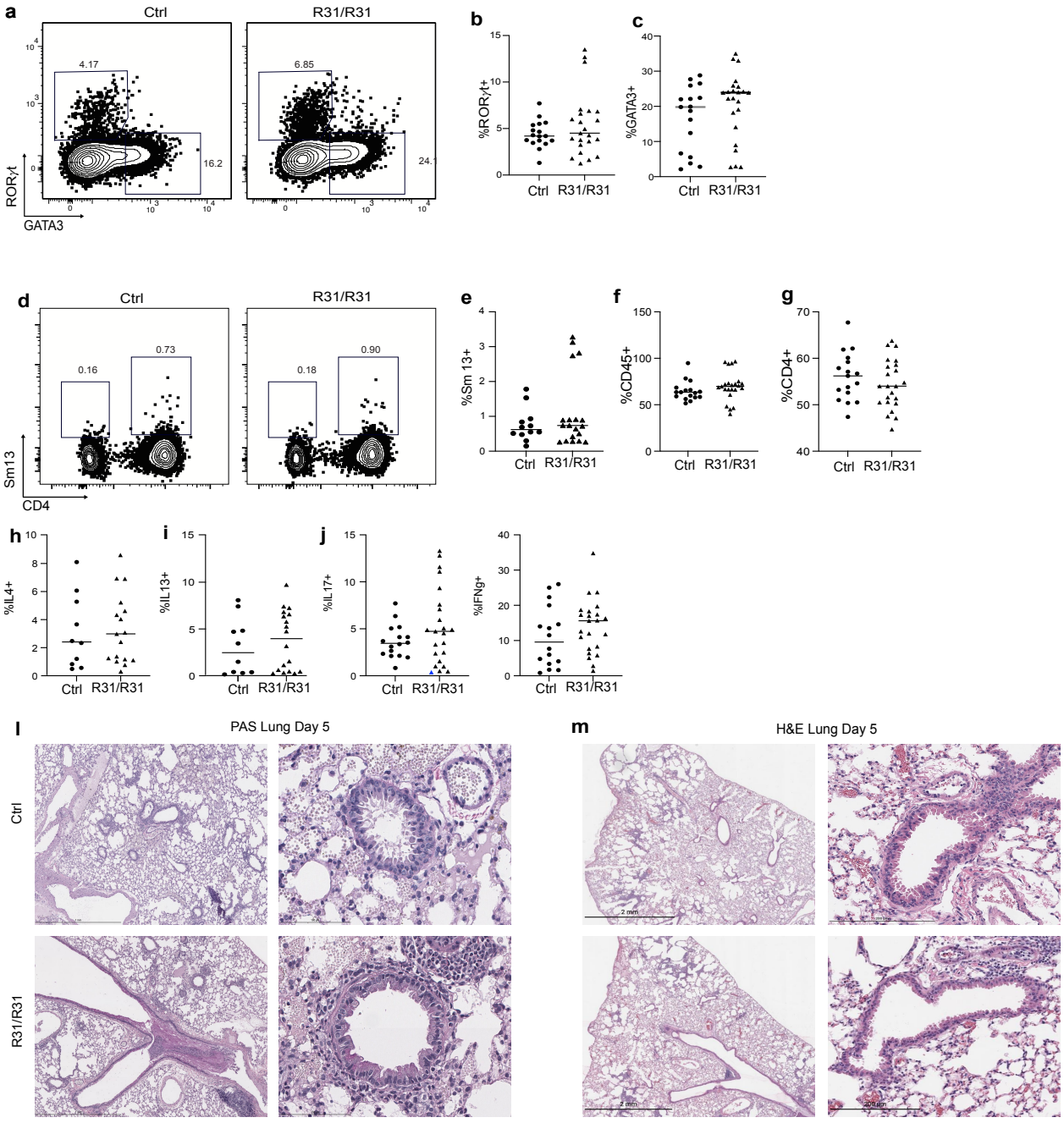

Supp Figure 2.1 Day 5 post Nb infection

(a) Representative FACS plot showing RORgt and GATA3 expression of CD3+C4+ T cells from N.b infected mice on day 5 (b,c) Quantification of RORgt and GATA3 expression of CD3+C4+ T cells from N.b infected mice on day 5 (h) Representative FACS plot of Sm13+CD4+ T cells from small intestine of N.b infected mice on day 5 (i) Quantification of Sm13+ (IL-13 reporter) CD4+ T cells from small intesting of N.b infected mice on day 5 (j,k) Quantification of CD45+ and CD4+ cell populations in the small intestine at day 5 post N,b infection (l) Periodic-Acid Schiff staining of small intestine at day 5. (m) Representative image of H&E stain of the small intestine on day 5.

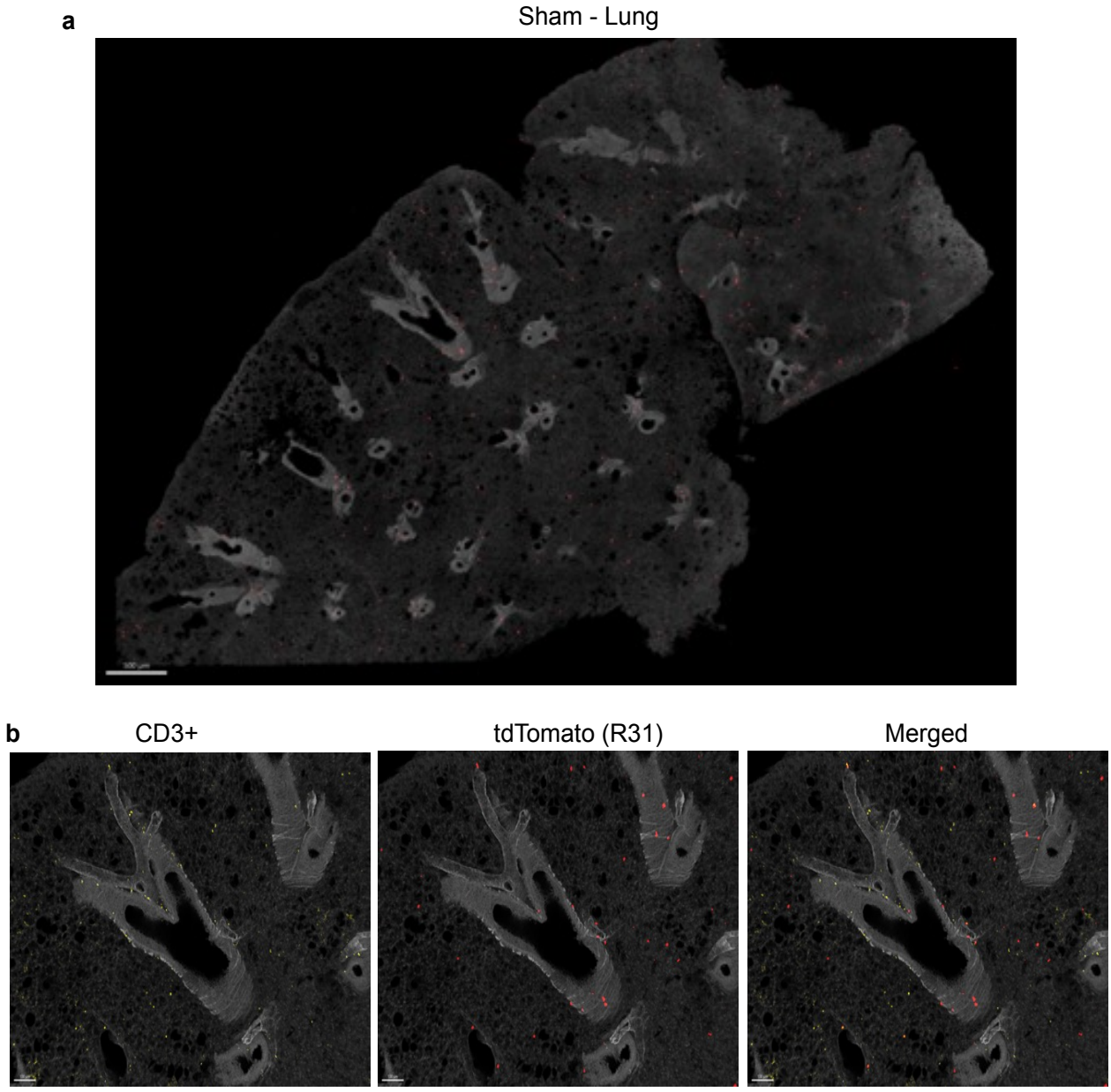

Supplemental Figure 2.2 Sham infected lung at day 5
(a) Representative immunofluorescence (IF) image of sham infected (PBS treated) right lobe of lung day 5 (b) 50μm zoom (IF) image of right lobe lung showing CD3 population (yellow, left), tdTomato (red, middle), and merged (orange, right)

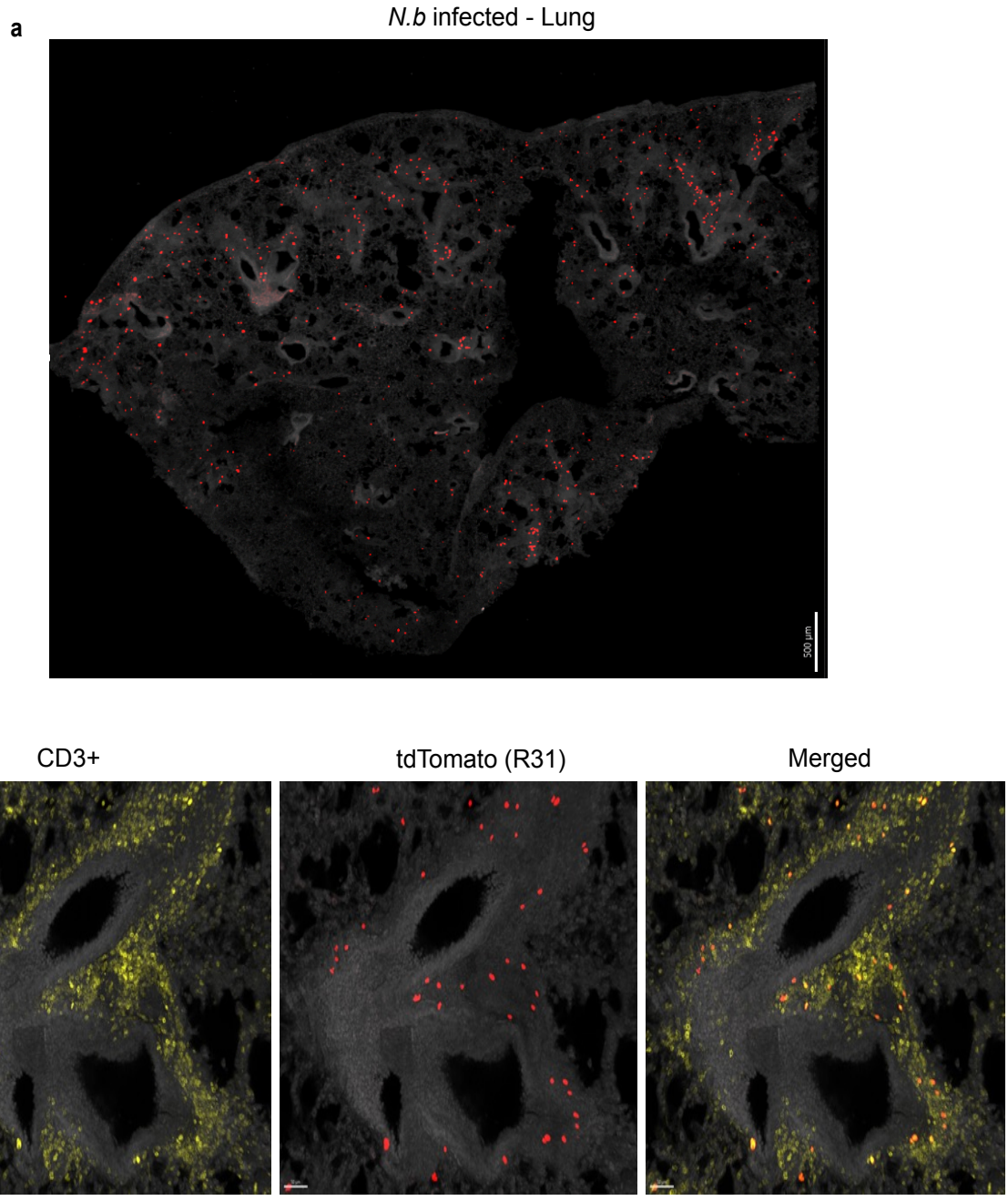

Supplemental Figure 2.3 *N.b* infected lung at day 5
(a) Representative immunofluorescence (IF) image of *N.b.* infected (PBS treated) right lobe of lung day 5 post *N.b* infection. (b) 50μm zoom (IF) image of right lobe lung showing CD3 population (yellow, left), tdTomato (red, middle), and merged (orange, right) after *N.b* infection

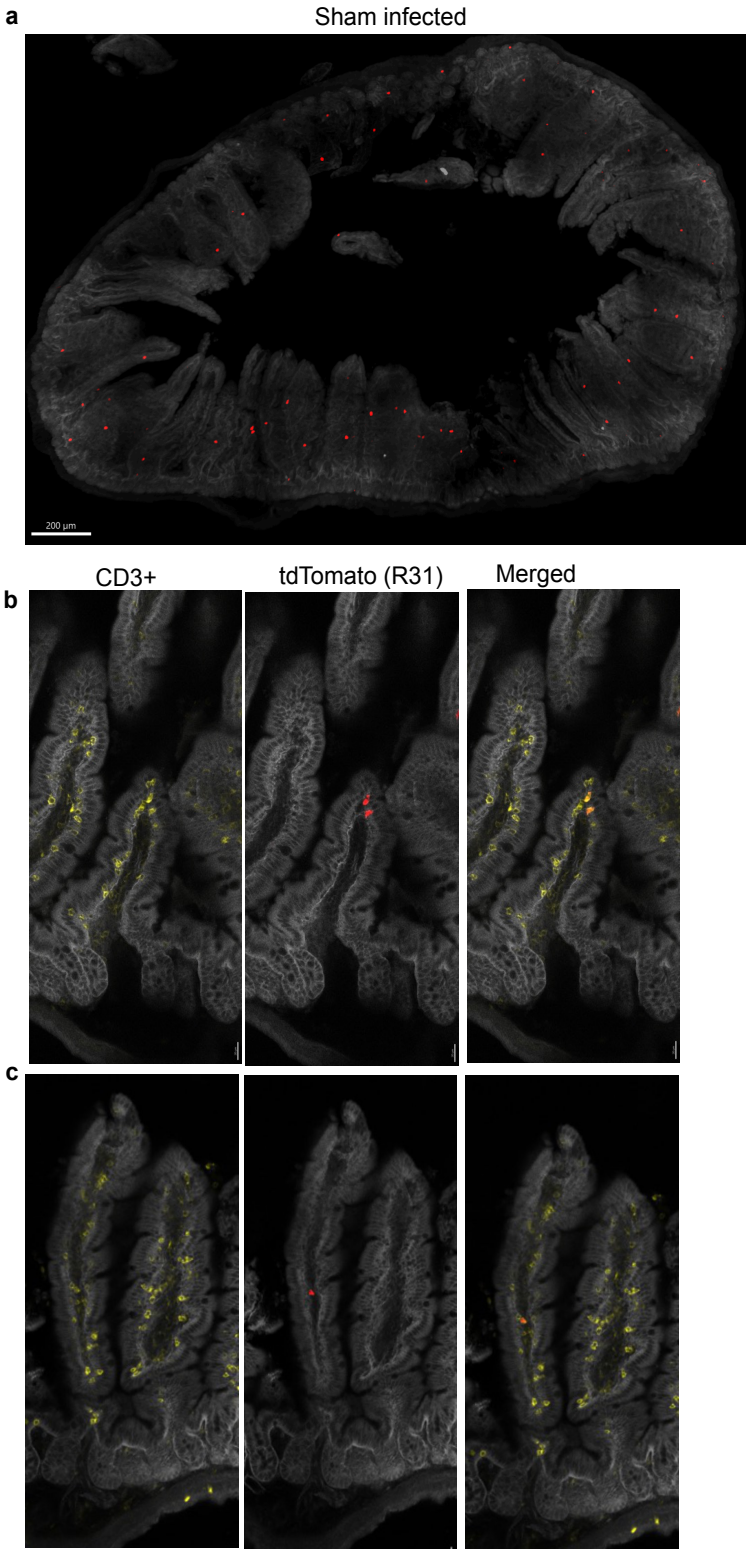

Supplemental Figure 2.4 Sham infected small intestine at day 5(a) Representative immunofluorescence (IF) image of sham treated small intestine (duodenal) section day 5 post *N.b* infection. (b) 50µm zoom (IF) image of small intestine (duodenal) section showing CD3 population (yellow, left), tdTomato (red, middle), and merged (orange, right) after *N.b* infection

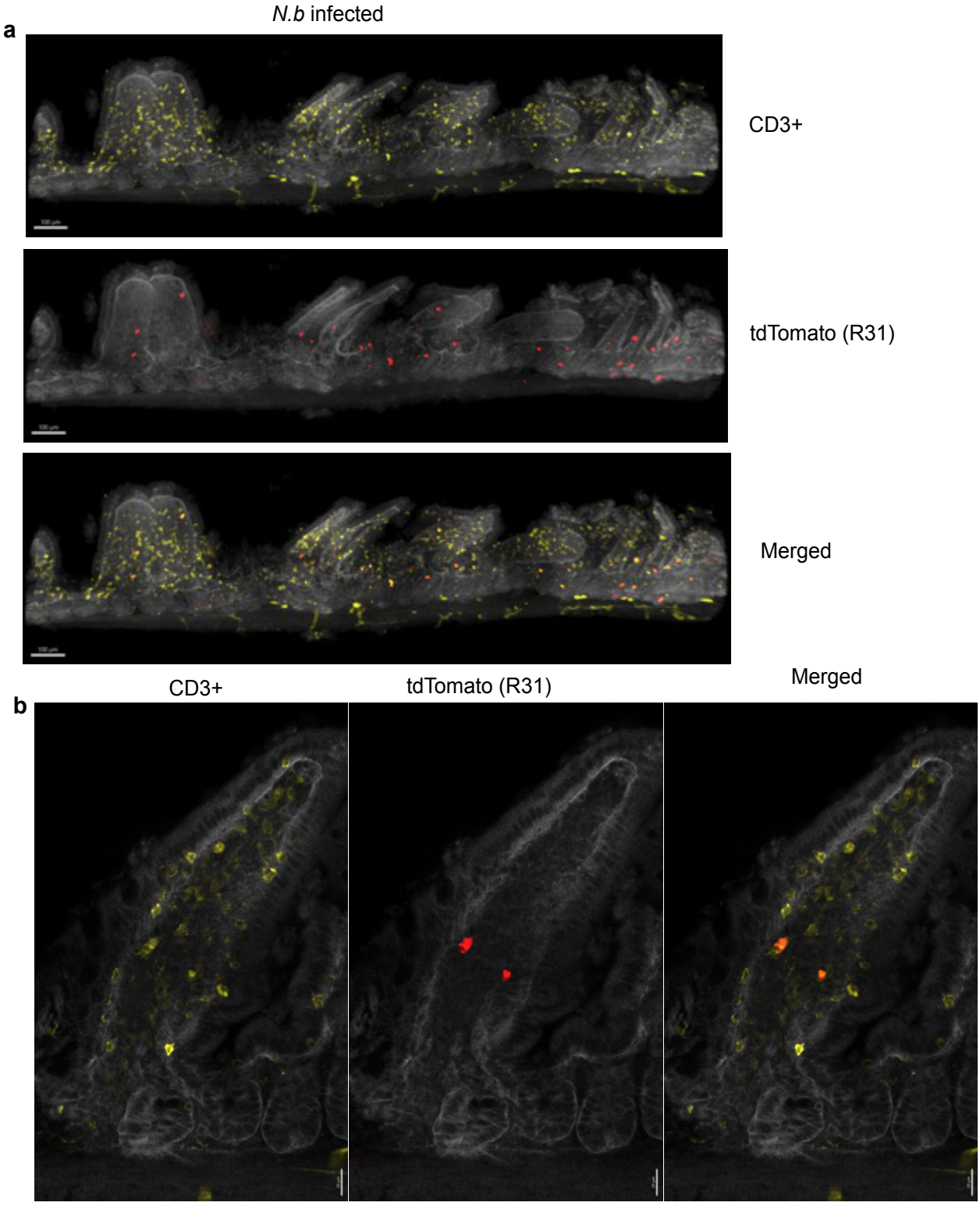

Supplemental Figure 2.5 *N.b* infected small intestine at day 5.
(a) Representative immunofluorescence (IF) image of *N.b.* infected small intestine (duodenal) section day 5 post *N.b* infection. (b) 50μm zoom (IF) image of small intestine (duodenal) section showing CD3 population (yellow, left), tdTomato (red, middle), and merged (orange, right) after *N.b* infection

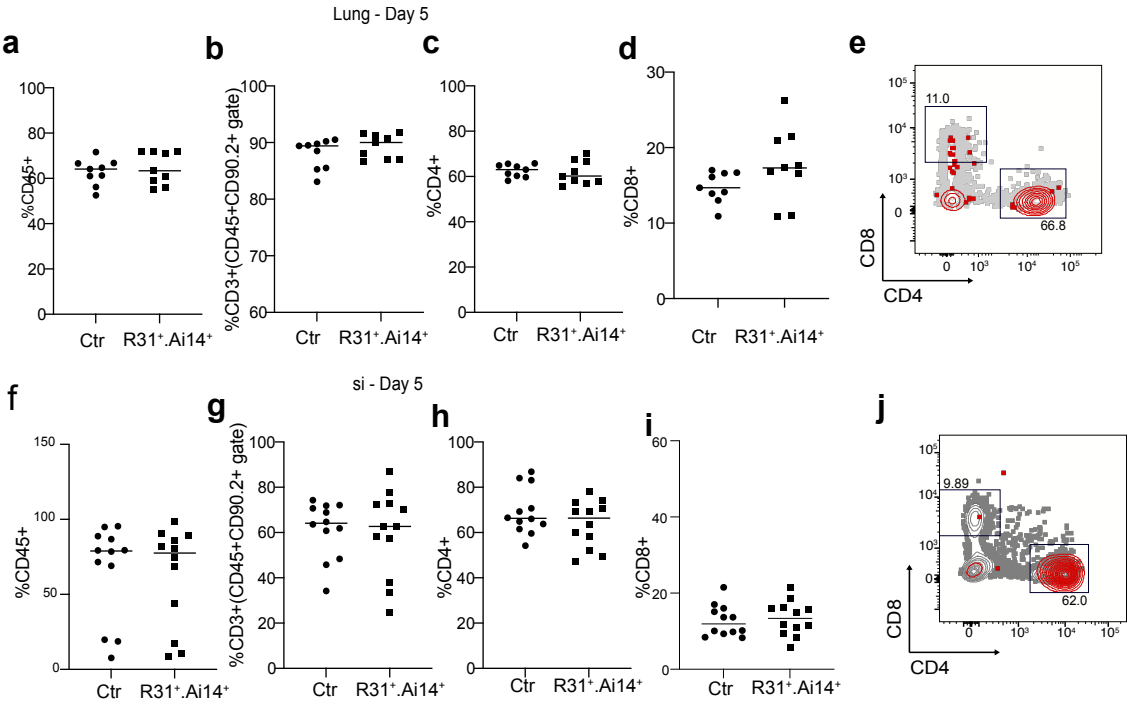

Supp Figure 2.6 Lymphocyte populations remain unchanged after day 5
(a, b, c, d) quantification of percentages of lymphoid cell population in the lung at day 5 post infection **(e)** FACS plot of CD3+ T cells, overall of Red31 reporter expressing CD4+ and CD8+ T cells over non-reporter expressing CD4+ CD8+ T cells in the lung**. (f, g, h, i)** quantification of percentages of lymphoid cell population in the gut at day 5 post infection **(j)** FACS plot of CD3+ T cells, overall of Red31 reporter expressing CD4+ and CD8+ T cells over non-reporter expressing CD4+ CD8+ T cells in the gut**.**

CHAPTER 3: MOLECULAR REGULATORS OF IL31 EXPRESSION

Introduction

These data show that the IL-31 – IL-31RA axis is important in the regulation of not only itch but also in moderating type 2 immune responses. However, the mechanisms that control the production of IL-31 remain largely understudied. *Il31* mRNA and IL-31 protein can be detected in the skin of patients with atopic dermatitis, but IL-31 levels do not always correlate with atopic dermatitis disease activity making it a poor biomarker for AD(Murdaca et al., 2019; Sonkoly et al., 2006). Thus far, NFAT, JunB and STAT6 have been implicated in *IL31* transcription (Hwang et al., 2015; Park et al., 2012). Investigation of patients with Dedicator of cytokinesis protein 8 (*DOCK8*) deficiency-related hyper IgE syndrome resulted in the discovery of an upstream regulation pathway of IL-31. DOCK8 loss-of-function mutations led to a combined immunodeficiency with elevated IgE serum levels, eosinophilia, decreased number of B and T cells, as well as severe atopic dermatitis with increased IL-31 expression(Yamamura et al., 2017). Based upon the variable levels of IL-31 in AD patient skin and data showing that IL-31 could promote type 2 immune responses it is very likely that there are additional inputs of IL31 transcription.

Results

Discovery And Validation Of IL-31 Regulators Using A Pooled CRISPR Screen

To identify potential regulators of IL-31, we used a pooled CRISPR-screening approach in primary mouse Th2 cells (**Fig. 3.1A**). A targeted library consisting of 20,000 single guide RNA (sgRNA) sequences that target transcription factors, kinases, phosphatases and metabolism-associated genes was generated from the Brie library (Doench et al., 2016). We used a retroviral vector with a Thy1.1 transduction marker gene to introduce

the library into T cells isolated fromR31.IL13^{Sm}Cas9^{GFP} (Platt et al., 2014) mice that were cultured *in vitro* under Th2 differentiation conditions. Using FACS to select for GFP+ Cas9-transgenic Thy1.1+ retrovirally infected cells, we sorted the highest (R31^{high}) and lowest (R31^{low}) R31-expressing cells (**Fig. 3.1A**). sgRNA sequences were amplified and sequenced from each population, and analyzed with MAGeCK software to systematically identify sgRNAs that were enriched or depleted in R31^{low} cells relative to R31^{high} cells. This screen revealed several regulators of R31 expression, including stromal interaction molecule 1 (*Stim1*) and interferon regulatory factor 4 (*Irf4*), (**Fig. 3.1B,C**). We also identified several other established regulators of other Th2 cytokines including *Il4ra and Satb1,* providing further confidence in our screen and hits. To validate the effects on R31 expression, we assessed ten of the top-ranking regulators by inducing individual CRISPR knockouts with T cell transfection with pre-assembled Cas9 ribonucleoproteins (RNPs) (Schuman, 2015). The effects on R31 expression were consistent across multiple guide RNAs targeting several candidate positive regulators (**Fig. 3.1D**).

The screen strongly identified *Stim1* as a positive regulator of IL-31. Cas9 RNPs targeting *Stim1* consistently and robustly decreased the expression of both R31 (**Fig. 3.2A,B**) and endogenous IL-31 protein (**Fig.3.2C,D**) in *in vitro* differentiated mouse Th2 cells. Production of IL-4 was also reduced (**Fig. 3.2C, E**). Since STIM1 functions as a calcium sensor in the endoplasmic reticulum (Zhang et al., 2005), we tested whether calcium signaling pathway inhibitors also affect IL-31 expression *in vitro* (**Fig.3.2 H**). We first assessed the role of calcium signaling in IL-31 expression by blocking calcium release-activated channels (CRAC), which are plasma membrane store-operated calcium entry (SOCE) channels opened by STIM when calcium ions are depleted from intracellular

stores in the endoplasmic reticulum. The SOCE inhibitor BTP2 was previously shown to inhibit pro-inflammatory cytokine production from immune cells in vitro and in vivo (Meizoso-Huesca & Launikonis, 2021; Srikanth et al., 2012; Zhang et al., 2005). Primary mouse CD4 T cells were isolated and differentiated under Th2 conditions in vitro, then pretreated with or without BTP2 for 10 minutes before activation with the phorbol ester PMA and the calcium ionophore Ionomycin. BTP2 abrogated R31 reporter and endogenous IL-31 protein expression (**Fig.3.2I**). Cyclosporin A (CsA) inhibits calcineurin, a calcium-dependent phosphatase that acts downstream of SOCE to regulate the localization of NFAT, a critical transcription factor for T cell activation and cytokine gene transcription (Luo, Burgeon, et al., 1996; Luo, Shaw, et al., 1996; Randak et al., 1990; Serafini et al., 1995). Like BTP2, CsA treatment completely blocked R31 reporter and IL-31 protein expression (**Fig. 3.2I**, right), consistent with prior evidence that CsA inhibits *Il31* mRNA expression in CD4+ T cells (Hwang et al., 2015). As expected, the production of the canonical Th2 cytokines IL-4 and IL-13 were also completely blocked by pretreatment with CSA or BTP2 (**Fig 4J**). Together these findings substantiate the results of our screen by confirming an upstream pathway involved in IL-31 expression.

IRF4 Negatively Regulates The Expression Of IL-31 In Mouse Th2 Cells

The transcription factor IRF4 was the most potent negative regulator of R31 identified in the screen. To further define the role of IRF4 in IL-31 expression, we targeted *Irf4* using Cas9 RNPs transfection in *Red31* transgenic T cells cultured under Th2 differentiation conditions. Targeting *Irf4* induced a robust increase in R31 reporter expression compared to the non-targeting sgRNA control (**Fig 3.3A,B**). In WT Th2 cells, we observed a 3-fold increase in the frequency of IL-31 protein production by *Irf4* targeted cells compared to a

non-targeting sgRNA control (**Fig. 3.3C,D**), demonstrating that IRF4 regulates endogenous IL-31 expression as well. This increase in IL-31 was not correlated with any significant change in the production of the canonical Th2 cytokines, IL-4 (**Fig. 3.3C,E**) or IL-13 (**Fig. 3.3F,G**). Intracellular co-staining for IRF4 and IL-31 showed the efficiency of *Irf4* sgRNA targeting in transfected cells and revealed selective production of IL-31 by $IRF4^{-}$ cells (**Fig. 5H**). Cell proliferation was also unaffected by *Irf4* sgRNA compared with non-targeting control sgRNA in Th2 differentiation cultures (**Fig. 3.3I**). These data demonstrate that IL-31, a cytokine previously described to be primarily secreted by Th2 cells, is subject to regulatory mechanisms distinct from those that control the expression of canonical Th2 cytokines.

We sought to understand the cell-intrinsic impact of *Irf4* on *Il31* expression. To do so, we performed the necessary crosses to generate transgenic mice that carry one copy of the *R31* transgene, which encodes a humanized Cre recombinase element (*hCre*, see **Fig 2.1A**), and two floxed *Irf4* alleles (B6.129S1-*Irf4*^{tm1Rdf}/J) (Klein et al., 2006). This combination of transgenes (*R31.Irf4*$^{flox/flox}$) drives selective, conditional deletion of *Irf4* only in cells that have ever expressed *Il31* (**Fig.3.3I**). In *in vitro* Th2-polarized CD4 T cell cultures, *R31*+ cell-specific *Irf4* deletion (R31.*Irf4*$^{fl/fl}$) resulted in 2-fold increases in *R31* reporter transgene expression compared to *Irf4* WT controls (**Fig 3.3J,K**)**.** Th2 cultures of cells that carried one functional copy of *Irf4 (R31.Irf4*$^{flox/WT}$) resulted in intermediate *R31*+ expression, indicating *Irf4* mediates dose-dependent repression of *Il31* (**Fig. 3.3K).**

To determine the effects of *Irf4* deletion in IL-31 expressing cells *in vivo*, we inoculated mice with *N.brasiliensis* and assessed worm burden at Day 7 (**Fig. 3.3L**). R31.Irf4$^{fl/fl}$ mice

showed a significant retention of worms in the siLP compared to control (**Fig. 3.3M**). These data suggest that an increase in IL-31 expression, driven by the absence of *Irf4* in IL-31 expressing cells, was sufficient to increase worm intestinal burden, a phenotype complementary to the accelerated worm clearance of *Il31*-deficient mice (**Fig. 2.1D**). Together, these data support an important role for *Irf4* regulation of IL-31 both *in vitro* and *in vivo*.

IRF4 Negatively Regulates The Expression Of IL-31 In Human Th2 Cells

To test whether IRF4 also functions as a negative regulator of *IL31* in primary human T cells, we targeted *Irf4* using Cas9 RNP transfection of CD4+ T cells isolated from peripheral blood mononuclear cells (PBMCs) and cultured *in vitro* under Th2 differentiation conditions (**Fig 3.4A**). Control cells were targeted at the safe harbor locus AAVS1, as disruption of this locus does not affect T cell growth or differentiation (Carnevale et al., 2022; Hayashi et al., 2020). We also targeted the *IL31* coding region as a positive control for loss of IL-31 expression. Transfected cells from several donors were restimulated on day 13 to induce cytokine production and processed for intracellular cytokine staining and flow cytometry to assess IL-31, IL-4 and IL-13 (**Fig. 3.4B-F**).

We observed robust Th2 differentiation, as indicated by IL-4 production, in cells from most donors (**Fig. 3.4B,C**). Less than 5% of AAVS1-targeted control Th2 cells produced IL-31. However, the proportion of IL-31 producing cells was significantly increased when the same cells were targeted using the *Irf4* sgRNA, with some donors having a 5-fold difference in IL-31 producing cells (**Fig. 3.4B,C**). Targeting the *IL31* coding region reduced IL-31 production as expected, with no effect on IL-4 production (**Fig 6B-D**). Targeting *Irf4*

modestly increased the proportion of IL-4 producing cells (**Fig. 3.4B,C**) but decreased IL-13 producing cells in most donors, despite considerable variability (**Fig. 3.4E,F**). Intracellular staining for transcription factors showed that sgRNAs targeting *Irf4* induced loss of IRF4 protein in a fraction of electroporated cells, and that those same cells expressed lower quantities of GATA3 (**Fig. 3.4G**), consistent with previous reports that IRF4 induces GATA3 in Th2 cells(Ahyi et al., 2009; Krishnamoorthy et al., 2017). Taken together, these data demonstrate that IRF4 is a potent negative regulator of IL-31 production, and that this function is conserved in mouse and human Th2 cells.

Discussion

While other groups also reported increased type 2 inflammation and/or type 2 cytokine production in the absence of *Il31* (Bilsborough et al., 2010; Perrigoue et al., 2007, 2009), this observation remains confusing because CD4 T cells are a key source of canonical type 2 cytokines IL-4 and IL-13. In fact, very little is known about what regulates IL-31 production in T cells. Now, with the *Red31* transgene available as a sortable marker in live cells, we were able to apply CRISPR screening technology for discovery of factors that activate or repress *Il31* production.

The high-throughput molecular screen we performed to identify activators and repressors of *Red31*(*Il31)* production in T cells. This approach successfully highlighted multiple *Il31* regulators with clear biological relevance to type 2 inflammation, including candidate genes for which concordant molecular or clinical data exists.

One notable example is *Il4ra*, a subunit common to both type I and type II IL-4 cytokine receptors and the pharmacologic target of dupilumab (Chang & Nadeau, 2017), which we identified as a positive regulator of *Il31*. These data indicate that signaling by one or both IL-4 receptor ligands (IL-4 or IL-13) is required for *Il31* production and suggest that pharmacological inhibition of *IL4RA* in atopic dermatitis patients is likely to reduce *IL31* production too (Chang & Nadeau, 2017b; Chiricozzi et al., 2020). Our finding accords with a known IL-4 signaling requirement for *IL31* transcription(Maier et al., 2014; Stott et al., 2013), and clinical data showing reduced serum IL-31 in dupilumab-treated atopic dermatitis patients (Kishi et al., 2023). Similarly, our CRISPR screen highlighted calcium signaling requirements for mouse *Il31* production. *Il31* transcription required *Stim1*, which encodes an endoplasmic reticulum calcium sensor required for store operated calcium entry (SOCE)-dependent calcium signaling (Gwack et al., 2007; Vaeth et al., 2020). Inhibitor studies confirmed that *Il31* production requires multiple nodes in the pathway from ER calcium flux to NFAT-mediated transcription. These results affirm previous molecular studies and clinical data showing serum IL-31 concentrations in AD patients decrease secondary to calcineurin-dependent NFAT dephosphorylation after cyclosporin treatment (Otsuka et al., 2011; Park et al., 2012).

In contrast, transcription factor *Irf4* repressed *Il31* production. The impressive magnitude of *Irf4* CRISPR editing on mouse *Il31* (up 2-fold) & its opposite directional effect on *Il4* was surprising given that co-expression of these cytokines in Th2 cells is frequently observed(Bilsborough et al., 2006; Fassett et al., 2023). In fact, *IRF4* is required for expression of Th2 lineage-specifying transcription factor *Gata3* and Th2 differentiation (Lohoff et al., 2002), which we observed in primary human Th2 cultures as decreases in

GATA3 and *IL4* expression in *IRF4*-edited (IRF4-low) cells. On this basis, one might predict a global decrease in Th2 differentiation would secondarily reduce *IL31* expression. However, that we observed the opposite – increased *IL31* expression in *IRF4*-edited cells – suggests an additional, *GATA3*- and *IL-4*-independent *IRF4* pathway also represses *IL31*. Our consistent evidence of *Irf4*-dependent *Il31* repression in mouse and human Th2 cells indicates that the *Irf4* mediated pathways that distinguish *Il31* repression from Th2 differentiation are evolutionarily conserved.

The organismal effect of *Irf4*-mediated *Il31* repression during an type 2 immune response to *Nb* is highlighted by our experiments in transgenic mice we engineered for selective *Irf4* deletion only in *Red31(Il31)*+ cells. During *Nb* infection these *Red31.Irf4*$^{fl/fl}$ mice produced more small intestinal *Il4/Il13*+ T cells and by day 5 harbored fewer *Nb* worms, a near-phenocopy of global *Il31KO* mice infected with *Nb*. This result is particularly striking if one considers two facts about *Red31.Irf4*$^{fl/fl}$ mice: First, that abundant populations of type 2 and *Irf4*+ lymphoid and myeloid lineage cells are unaffected by *Red31* cell-specific *Irf4* deletion. Second, that *Red31(Il31*)-expressing cells are very rare in uninfected animals, and only modestly increase in lung and small intestine in the setting of *Nb* infection. Clearly, we have much to learn about the *in vivo* biology and potent immunoregulatory effects of these under-detected and under-appreciated cells.

Methods

In Vitro Cell Cultures

Primary CD4+ mouse T cells were isolated from mouse peripheral lymph nodes and spleen using EasySep Mouse CD4 Negative Isolation Kit (StemCell Technologies) according tothe manufacturer's instructions. Cells were stimulated with immobilized biotinylated anti-CD3 84(clone 2C11, 0.25 µg/mL, BioXcell) and anti-CD28 (clone 37.51, 1 µg/mL, BioXcell) bound to Corning cell culture dishes coated with Neutravidin (Thermo) at 10 µg/mL in PBS for 3 h at 37°C. Cells were left on stimulation and treated with 10µg/mL of anti-interferon gamma (αIFNγ) and IL-4 supernatant for 3 days before being transferred to non-coated dishes in T cell medium supplemented with recombinant human IL-2 (20 U/mL) and 10µg/mL of αIFNγ . For re-stimulation, cells were treated with 20nM phorbol 12-myristate 12-acetate (PMA) and 1 µM ionomycin (Sigma) for 4hours before harvest.

CRISPR Editing of T cells

Guide RNA sequences were selected using the Benchling online CRISPR design tool (https://benchling.com/crispr) with guides selected to target genomic regions identified by the CRISPR screen. Synthetic crRNAs and tracrRNA (Dharmacon) were resuspended in water at 160 µM at 1:1 ratio and allowed to hybridize at 37 c for 30 m. This annealed gRNA complex (80 µM) was then mixed 1:1 by volume with 40 µM S. pyogenes Cas9-NLS (University of California Berkeley QB3 Macrolab) to a final concentration of 20 µM Cas9 ribonucleotide complex (RNP). The diluted gRNA:Cas9 RNPs along with a random 200bp single-stranded DNA fragment were nucleofected into primary human (48 hours after stimulation) or mouse CD4 T cells (24 hours after stimulation) with the P3 Primary Cell 96-well Nucleofector ™ Kit. Cells were pipetted into pre-warmed media and then

returned to anti-CD3 and anti-CD28 stimulation for another 2 days for primary mouse T cells or 1 day for primary human T cells . Unless otherwise stated, control-edited T cells were targeted with the AAVS1 sequence GGGCCACTAGGGACAGGAT.

Retrovirus production

Platinum-E (Plat-E) Retroviral Packaging cells (Cell Biolabs, Inc., Cat# RV-101) were seeded at 10 million cells in 15 cm poly-L-Lysine coated dishes 16 hours prior to transfection and cultured in complete DMEM, 10% FBS, 1% pen/strep, 1 µg/mL puromycin and 10 µg/mL blasticidin. Before transfection, the media was replaced with antibiotic free complete DMEM, 10% FBS. The cells were transfected with the sgRNA transfer plasmids (MSCV-U6-sgRNA-IRES-Thy1.1) using polybrene. The next day, the media was replaced with complete DMEM, 10% FBS, 1% pen/strep. The viral supernatant was collected 48 hours post transfection and filtered through a 0.45 µm, polyethersulfone sterile syringe filter (Whatman, Cat# 6780-2504), to remove cell debris. The viral supernatant was aliquoted and stored until use at -80°C.

Quantification and Statistical Analysis

Excel (Microsoft), Prism (GraphPad), Flowjo (TreeStar), MAGeCK(v0.5.7) were used for data analysis. Individual statistical tests performed are included in the data legends. All data was assumed to be normally distributed unless stated otherwise.

Figures

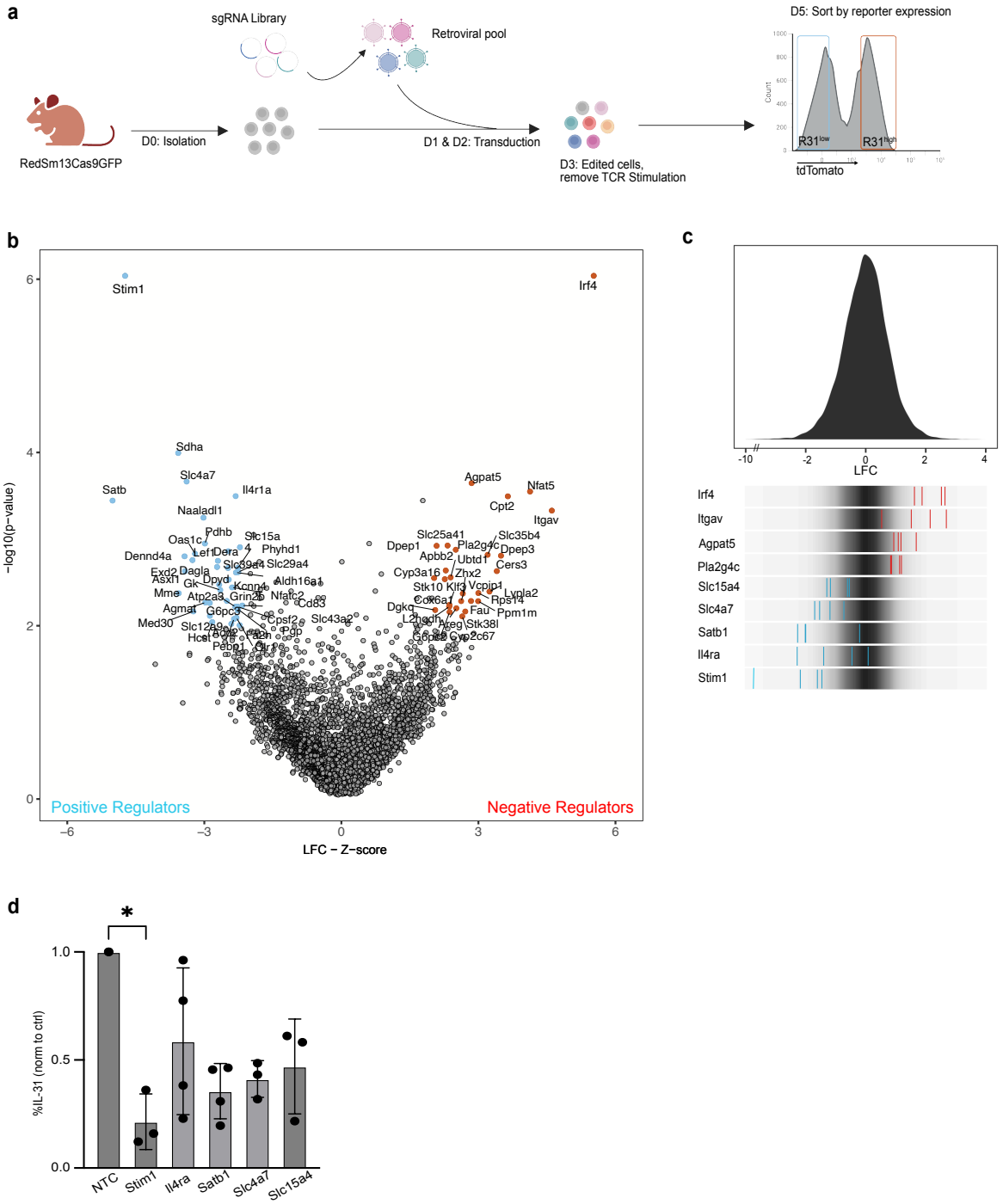

Figure 3.1 Discovery and validation of IL-31 regulators using a pooled CRISPR screen (a) schematic of experimental design for transduction of sgRNA library via CRISPR-Cas9 and selection via reporter expression **(b)** Volcano plot of CRISPR screen hits **(c)** Distribution of top guides **(d)** IL-31 expression by CD4+ T cells assessed via intracellular cytokine staining for positive regulators of IL-31

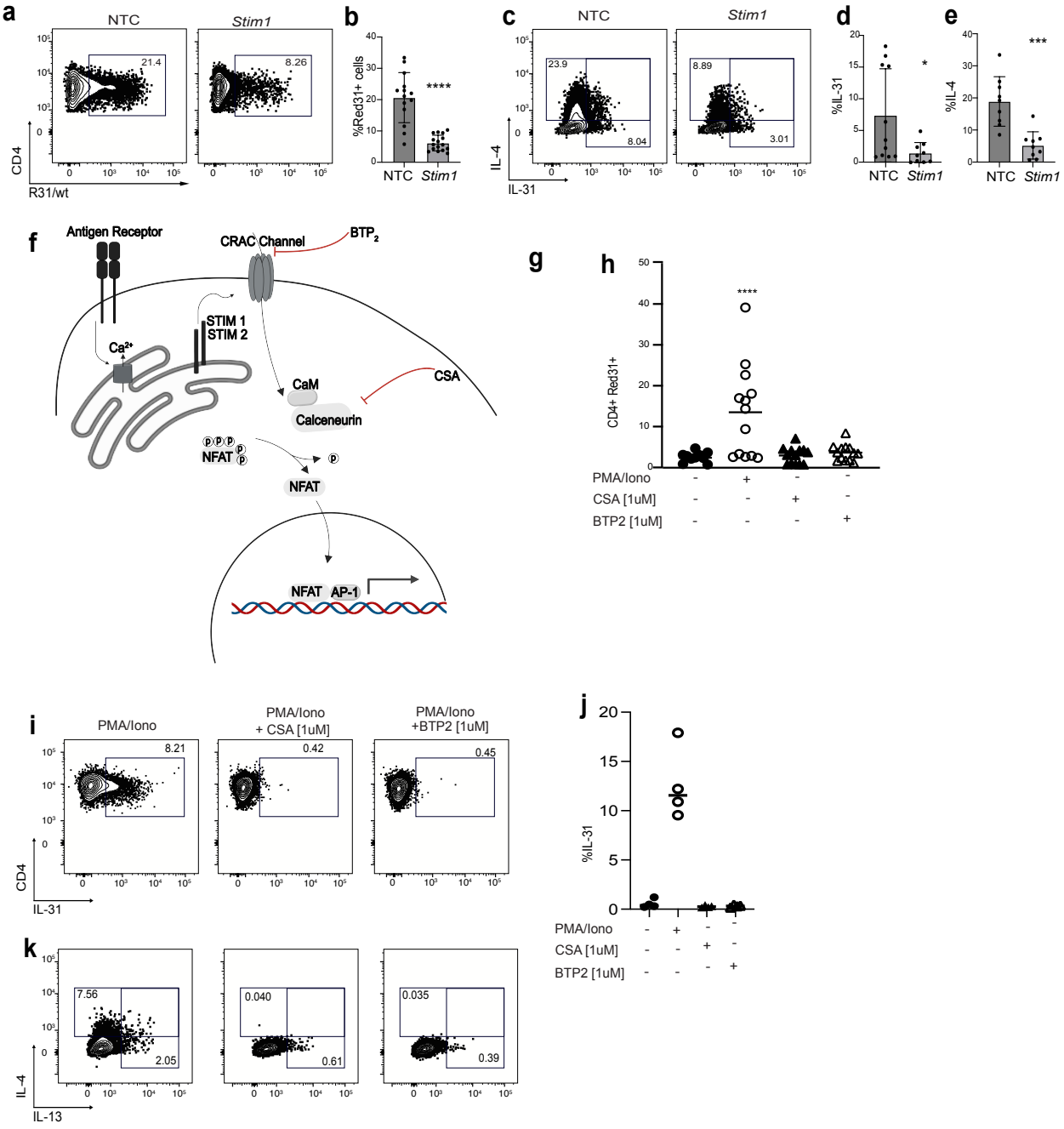

Figure 3.2 IL-31 expression is calcium dependent and is positively regulated by Stim1 (a) FACS plot of non-targeting control (NTC) and *Stim1* targeted CD4+ T cells, assessing Red31 reporter expression. (b) quantification of reporter expression from CD4+ T cells (c) FACS plot of non-targeting control (NTC) and *Stim1* targeted CD4+ T cells assessing IL-4 and IL-31 protein expression. (**d**), (**e**) quantification of IL-4 and IL-31 expression via intracellular cytokine staining of CD4+ T cells. (f) Schematic of calcium signaling and treatment with either CSA or BTP2 (h) Quantification of R31 expression from in vitro differentiated Th2 cells treated with CSA or BTP2 after stimulation with PMA and Ionomycin (i) FACS plot of IL-31 expression of CD4+ T cells

from in vitro differentiated Th2 cells treated with CSA or BTP2 after stimulation with PMA and Ionomycin. (j) quantification of IL-31 expression via intracellular cytokine staining of in vitro differentiated Th2 cells treated with CSA or BTP2 after stimulation with PMA and Ionomycin. (k) FACS plot of IL-4 and IL-13 expression by in vitro differentiated Th2 cells treated with CSA or BTP2 after stimulation with PMA and Ionomycin

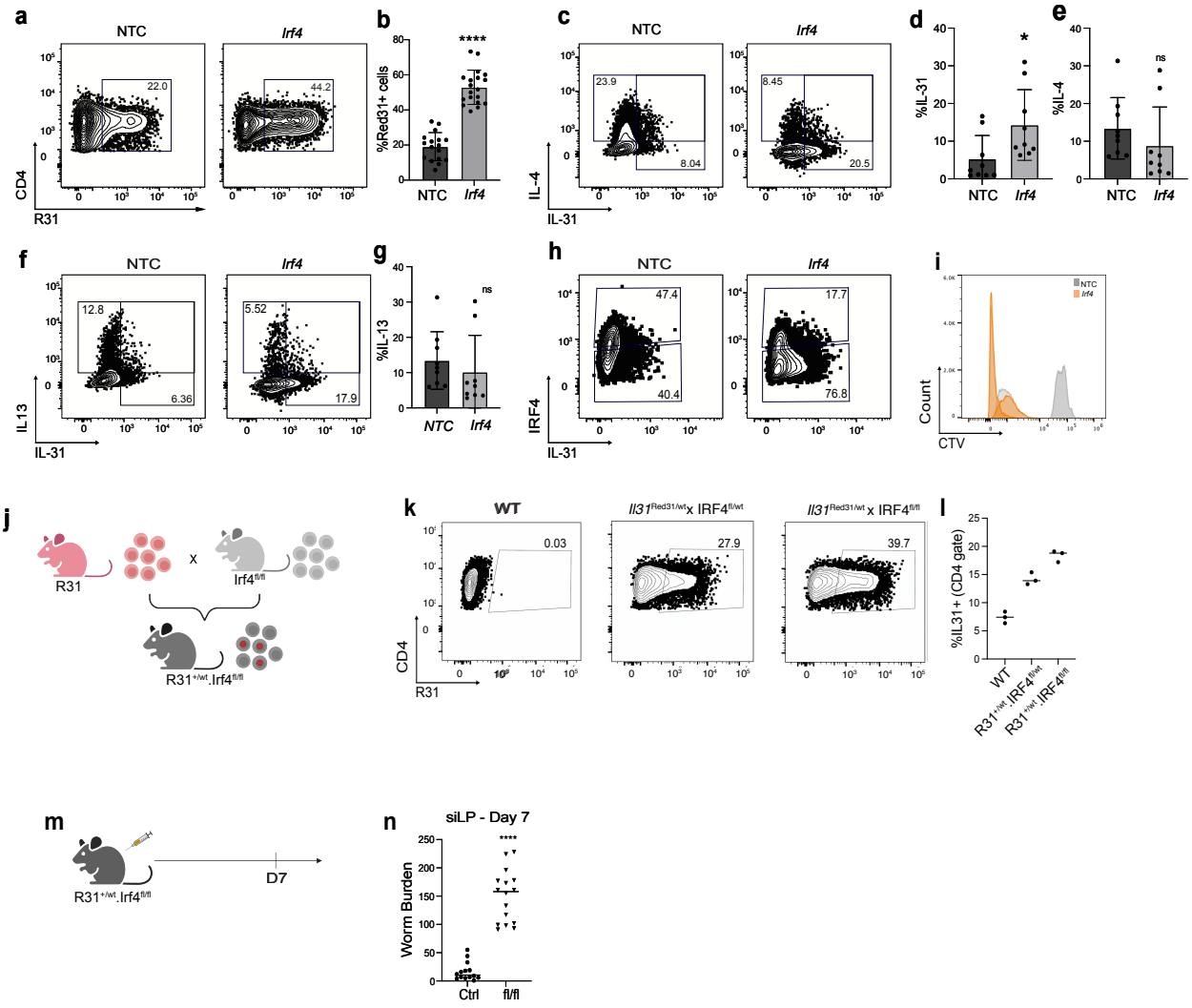

Figure 3.3 IRF4 negatively regulates the expression of IL-31 in mouse Th2 cells
(**a**) FACS plot of non-targeting control (NTC) and Irf4 targeted CD4+ T cells, assessing Red31 reporter expression. (**b**) quantification of reporter expression from CD4+ T cells. (**c**) FACS plot of non-targeting control (NTC) and Irf4 targeted CD4+ T cells assessing IL-4 and IL-31 protein expression. (**d**), (**e**) quantification of IL-4 and IL-31 expression via intracellular cytokine staining of CD4+ T cells. (**f**),(**g**) FACS plot and quantification of IL-13 and IL-31 expression via intracellular cytokine staining of CD4+ T cells. (**h**) FACS plot of IRF4 and IL-31 expression in NTC and Irf4 sgRNA targeted CD4+ T cells. (**i**) CTV labeling of NTC and Irf4 sgRNA targeted CD4+ T cells. (**j**) schematic of generation of Red31+/wt.Irf4fl/fl mice. (**k**) FACS plot of *in vitro* differentiated Th2 cells from Red31+/wt.Irf4fl/fl mice assessing R31 reporter expression. (**l**) quantification of IL-31 protein expression from *in vitro* differentiated Th2 cells from Red31+/wt.Irf4fl/fl mice. (**m**) schematic of N.b infection (**n**) quantification of worm burden of Red31+/wt.Irf4fl/fl mice

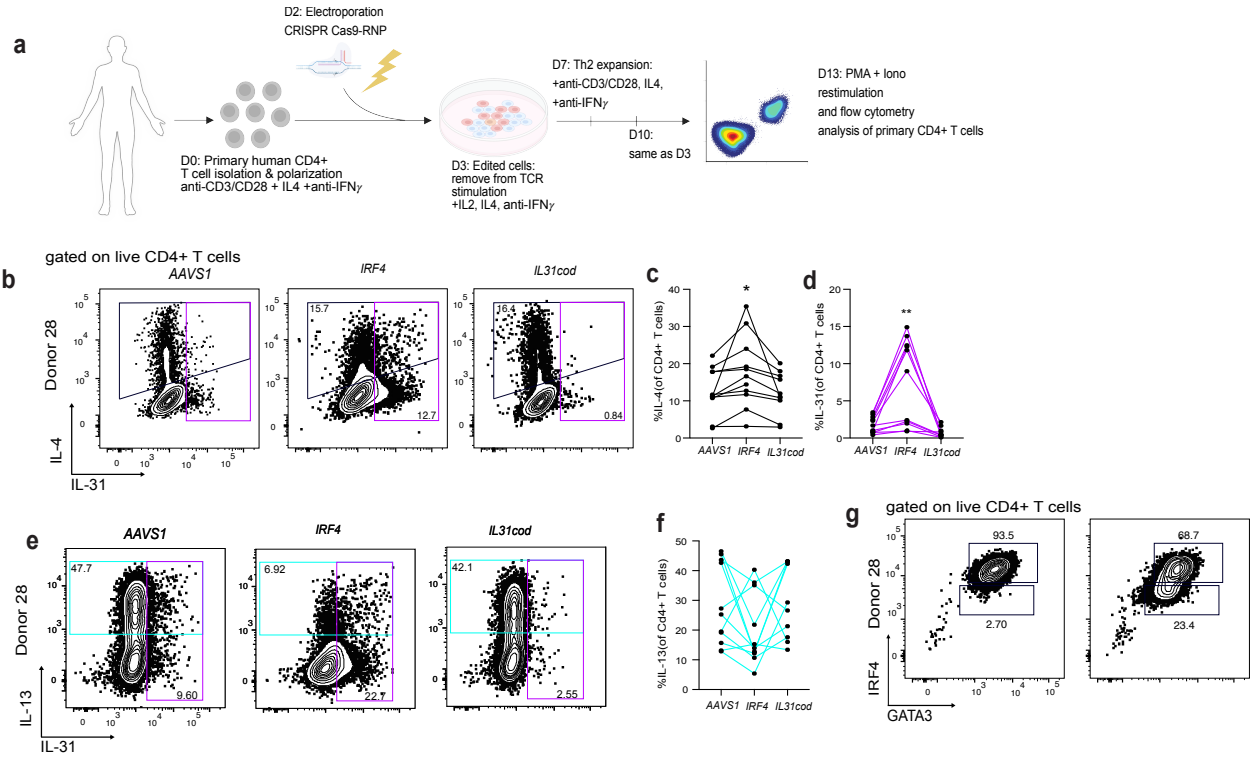

Figure 3.4 IRF4 negatively regulates the expression of IL-31 in human Th2 cells
(**a**) Schematic of polarization and introduction of CRISPR-Cas9 in to human Th2 cells. (**b**) Representative FACS plot of CD45+CD3+CD4+ T cells showing IL-4 and IL-13 expression. (**c**),(**d**) quantification of IL-4 and IL-31 from average of all donors. (**e**) Representative FACS plot of CD45+CD3+CD4+ T cells showing IL-31 and IL-13 expression. (**f**) quantification of IL-13 taken from average of all donors. (**g**) FACS plot of CD4+ T cells showing expression of IRF4 in AAVS1 v *Irf4* targeted Th2 cells

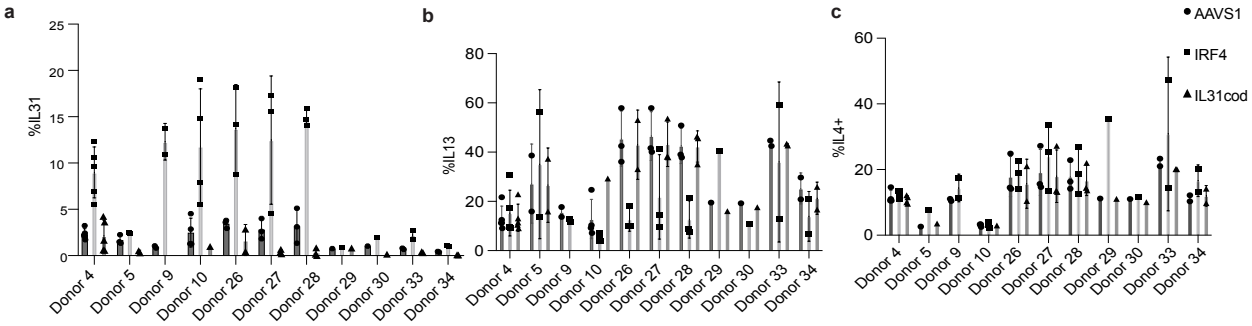

Figure 3.5 Cytokine expression of Th2 polarized human T cells edited with IRF4 crRNA (**a**) quantification of IL-31 expression by CD4+ T cells from each individual donor. (**b**) quantification of IL-13 by CD4+ T cells from each individual donor (**c**) quantification of IL-4 expression by CD4+ T cells from each individual donor

Tables

Table 3.1 Top 10 positive regulators

id	num	neg|score	neg|p-value	neg|fdr	neg|rank	neg|goodsgrna	neg|lfc	pos|score	pos|p-value	pos|fdr	pos|rank	pos|goodsgrna	pos|lfc
Stim1	4	1.77E-06	9.14E-07	0.00495	1	4	-1.8988	1	1	1	5415	0	-1.8988
Sdha	4	2.56E-05	0.000101	0.27475	2	4	-1.4345	0.99997	0.99996	1	5414	0	-1.4345
Slc4a7	4	5.94E-05	0.000217	0.38036	3	4	-1.3609	0.99994	0.99992	1	5413	0	-1.3609
Il4ra	4	8.98E-05	0.000319	0.38036	4	3	-0.9321	0.91582	0.9155	0.9999	4953	0	-0.9321
Satb1	4	0.0001	0.000359	0.38036	5	3	-2.0085	0.97367	0.97375	1	5254	0	-2.0085
Naaladl1	4	0.000151	0.000566	0.43777	6	3	-1.2135	0.68849	0.74088	0.9999	3974	1	-1.2135
Ikzf3	4	0.000239	0.000893	0.5374	7	2	-0.77448	0.28491	0.44448	0.9897	2331	2	-0.77448
Pdhb	4	0.0003	0.001125	0.54356	8	4	-1.2013	0.9997	0.99968	1	5412	0	-1.2013
Slc15a4	4	0.000334	0.001242	0.54356	9	4	-0.89478	0.99967	0.99966	1	5411	0	-0.89478
Dera	4	0.000376	0.00138	0.54356	10	4	-0.99632	0.99962	0.99962	1	5410	0	-0.99632

Table 3.2 Top 10 positive regulators

id	num	neg|score	neg|p-value	neg|fdr	neg|rank	neg|goodsgrna	neg|lfc	pos|score	pos|p-value	pos|fdr	pos|rank	pos|goodsgrna	pos|lfc
Irf4	4	1	1	0.999999	5415	0	2.199	1.93E-08	9.14E-07	0.00495	1	4	2.199
Agpat5	4	0.99994	0.99992	0.999999	5414	0	1.1313	6.35E-05	0.0002258	0.389109	2	4	1.1313
Nfat5	4	0.96706	0.96689	0.995381	5259	0	1.6423	7.89E-05	0.0002825	0.389109	3	3	1.6423
Cpt2	4	0.91854	0.91817	0.993402	4998	0	1.448	9.22E-05	0.0003209	0.389109	4	3	1.448
B4galnt1	4	0.26651	0.42146	0.993402	2151	1	0.7048	0.00010011	0.0003593	0.389109	5	3	0.7048
Itgav	4	0.99817	0.99981	0.999999	5401	0	1.8325	0.00012688	0.000469	0.423267	6	4	1.8325
Pla2g2e	4	0.47429	0.62337	0.993402	3220	1	0.2355	0.00030031	0.0011272	0.701733	7	2	0.2355
Slc25a41	4	0.99968	0.99968	0.999999	5413	0	0.92102	0.00031695	0.0011876	0.701733	8	4	0.92102
Dpep1	4	0.99968	0.99967	0.999999	5412	0	0.82495	0.00032077	0.0011949	0.701733	9	4	0.82495
Pla2g4c	4	0.99964	0.99964	0.999999	5411	0	0.99269	0.00035883	0.0013265	0.701733	10	4	0.99269

Table 3.3 List of crRNA

Species	Guide_Name	Sequence
Mouse	Sdha_1	GTCAGTTACCTCAACCACAG
Mouse	Sdha_2	TTCTACTCAATACCCAGTGG
Mouse	Sdha_3	TGCACAGTGCAATGACACCA
Mouse	Sdha_4	ACTGTGCATTACAACATGGG
Mouse	Slc4a7_1	TCAGGAACATAAGGTCCATG
Mouse	Slc4a7_2	TCTGCAAAGGATCGAACCAG
Mouse	Slc4a7_3	ACAGTATAGGAAAAGAATCG
Mouse	Slc4a7_4	GCAGATCCATTAGGAAACAC
Mouse	Il4ra_2	CACTAACATTCTCTGGCCAG
Mouse	Il4ra_3	ATCCAGGAACCACTCACACG
Mouse	Il4ra_4	CAGGATTAAGAAGATATGGT
Mouse	Satb1_2	GCAAGTTTCCACAAACACGG
Mouse	Satb1_3	GGAGTGCCTTTAAAACACTC
Mouse	Satb1_4	AGAAATTCTGCATAGCCCGA
Mouse	Naaladl1_2	GGAAATCCTGAGGTGTTGTG
Mouse	Naaladl1_3	AGTGGAAGGTTGTTCCATTG
Mouse	Naaladl1_4	TGGCTCTACAGAATTTACAG
Mouse	Ikzf3_1	GACAACAGCAGACCAACCGG
Mouse	Ikzf3_2	TAACGCCATCAGCTATCTAG
Mouse	Pdhb_1	TCTTAATTGTAGGTTAGCAG
Mouse	Pdhb_2	GGGCACAGGCTGAAGGCCAG
Mouse	Pdhb_3	TGAAGCTATTAATCAAGGTA
Mouse	Pdhb_4	GCCATTCGTGATAATAACCC
Mouse	Slc15a4_1	GCGTGGAGGGCCGTTCACAG
Mouse	Slc15a4_2	GACACGACGCTGACCCGTTG
Mouse	Slc15a4_3	TATCACCACCACCCATCACA
Mouse	Slc15a4_4	CCAATTGAAAAATCTCCGAG
Mouse	Dera_1	TGAGGTCACTCAGTTTCGAA
Mouse	Dera_2	AAGTCTTACCTGAGGCCACG
Mouse	Dera_3	AGTCTGCGTTTATCCCGCCC
Mouse	Dera_4	CGTGGTCATTAACAGGACCT
Mouse	Agpat5_1	GCAAAGTAGAACCCATACAG
Mouse	Agpat5_2	CTGCAGAGCTATGTGAACGC
Mouse	Agpat5_3	TGCAATTTATGATGTCACAG
Mouse	Agpat5_4	CAGGCATTTGCTGCTCAGCG
Mouse	Nfat5_1	TCAGCCATTTACGTACACTC
Mouse	Nfat5_3	GCCGTGGGGGTAAGTAACAG
Mouse	Nfat5_4	AAGACCAACTTCTATAACAG

Species	Guide_Name	Sequence
Mouse	Cpt2_2	TCGGGAAGTCATCTAAGCAG
Mouse	Cpt2_3	AAATATTGGGACATATCCAG
Mouse	Cpt2_4	TTAAATACATATCAAACCAG
Mouse	B4galnt1_1	TCTAGCAGATCGAGTCTCGG
Mouse	B4galnt1_2	TGACCGTAGGGTAAAAGCGT
Mouse	B4galnt1_4	TGCAGTTGTGAATCCAAGGG
Mouse	Itgav_1	GGTGCCATCTCAAATCCTCG
Mouse	Itgav_2	TCATGGACCGAGGTTCCGAT
Mouse	Itgav_3	CCTGCATGGAGCATACTCAA
Mouse	Itgav_4	ATAATAACCAATTAGCAACA
Mouse	Pla2g2e_2	GCCATAGTCATTGTACTGCA
Mouse	Pla2g2e_4	TATGGCTGCTATTGCGGTGT
Mouse	Slc25a41_1	GACGCTCATAAACCCCATGG
Mouse	Slc25a41_2	CTAGGTCGGTGCAAGCATAG
Mouse	Slc25a41_3	GAACTTGATAGCATACTCTG
Mouse	Slc25a41_4	ACAAACCTGCATGTACACCC
Mouse	Dpep1_1	TCACCCGTCGATGACCGGTG
Mouse	Dpep1_2	GACAACTGGCTTGTGGACAG
Mouse	Dpep1_3	AGTGGCCAGTCTGATCGGCG
Mouse	Dpep1_4	ATGTATGCGGACCAGAACTG
Mouse	Pla2g4c_1	GCACACCAAGACAAGCGATG
Mouse	Pla2g4c_2	TTTCATTCACAAAAACGCAA
Mouse	Pla2g4c_3	AGAGATTTGACTTTCCTGAG
Mouse	Pla2g4c_4	AGAAGCACCAAGGATGAATG
Mouse	Irf4_1	CAAGCAGGACTACAATCGTG
Mouse	Irf4_2	ACCTTATGCTTGGCTCAATG
Mouse	Irf4_3	GGTGTACAGGATTGTTCCAG
Mouse	Irf4_4	CCTGTGACGTTTGGCCCACG
Mouse	Stim1_1	TGAGGATAAGCTTATCAGCG
Mouse	Stim1_2	GAATACAGGAGCTAGCTCCG
Mouse	Stim1_3	GAGCCGTCAAAAATATGCTG
Mouse	Stim1_4	CAGCAGATCGAGATCCTCTG
Human	huIRF4_1	GGAAATCCCGTACCAATGTC
Human	huIRF4_2	CTGATCGACCAGATCGACAG
Human	huIRF4_3	GTGTACAGGATTGTTCCTGA
Human	huIL31cod_1	aacaacatccacagcccagc
Human	huIL31cod_2	agaattacacgctgccgtgt
Human	huIL31cod_3	cagagtgcatggacctcgcac

CHAPTER 4: CONCLUDING REMARKS

Future Directions

This body of work attempted to first, further elucidate the impact of IL-31 on type 2 immune response and second, study the molecular regulation of Il31 expression via discovery approach. In assessing the role of IL-31 in a type 2 immune response we used a helminth model that would allow us to study immune cell populations and activation in both the lung and the gut. In these tissues, observed an expansion of IL-31 expressing cells in the lung but no differences in cytokine profile while in the gut we observed minimal expansion of IL-31 expressing cells but a robust difference in cytokine expression and inflammation in the absence of IL-31. It would be of importance to study which cell types respond to IL-31 to further understand gut and lung allergic conditions as well as the effects of IL-31 blockade.

The CRISPR screen revealed a novel negative regulator of *Il31* expression both in mouse and human Th2 cells, *Irf4.* There were many other targets that were discovered as a result of the screen, although there were attempts to further study the biology of some of the targets that were identified by the screen many were left for further investigation. One such attempt at further understanding regulation of *Il31* was assessing the role of integrin alpha V, *Itgav*, as a negative regulator of IL-31. In Th2 differentiated cultures treated with RMV7, blocking antibody for alpha V, we saw an upregulation of R31 reporter expression compared to non-targeting controls (**Fig. 4.1 a,b,c**) and observed morphological changes in the amount of clumping and adhesion of Th2 cultures (**Fig. 4.2 d**). We also assessed whether upstream alarmins, TSLP and IL-33, impacted IL-31 expression. We observed

that IL-33, which signals through the NFkB pathway, and not TSLPE upregulated R31, reporter expression in in vitro differentiated Th2 cells (**Fig. 4.2 a, b, c,d**).

There is a 30% homology between the mouse and human *Il31* gene. Our screen identified *Irf4* as a negative regulator of IL-31 in mouse Th2 cells. Our study determined that *Irf4* is also a negative regulator of IL-31 in human Th2 cells. Given that information we looked for regulatory regions upstream of the human Il31 gene and found a region containing a DNase hypersensitive site, ATACseq peak (Henriksson et al., 2019)and within that region a potential NFkB and Irf4 transcription binding site (**Fig. 4.3 a**). We used CRISPR-Cas9 crRNAs to target that distal regulatory region and assessed IL-31 expression (**Table 4.1**). IL-31 expression was reduced compared to AAVS1 control Th2 cells (**Fig. 4.3 b,c**). This identifies another region that positively regulated IL-31 in human Th2 cells. This suggests that we can further study differences and similarities in the regulation of IL-31 expression in mouse and human Th2 cells, determine whether these mechanisms differ in other cell types, and provide other targets that would not have side effects of exacerbated asthma and gastroenteritis.

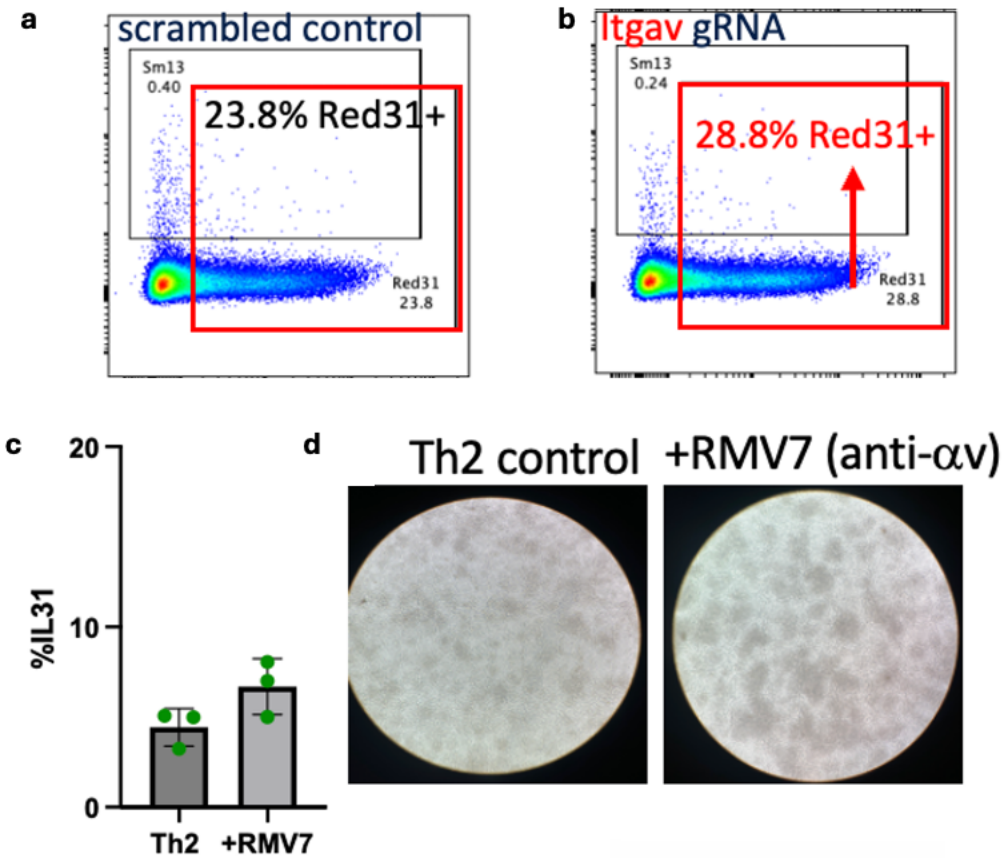

Figure 4.1 Itgav blockaged increases IL-31 expression and changes morphology of Th2 cell cultures
(a,b) Representative FACS plot of in vitro differentiated Th2 cells showing Sm13 (IL-13 reporter) and R31 reporter expression after treatment with RMV7 (b) Quantification of IL-31 expression (c) Representative images of in vitro differentiated Th2 cultures at day 5

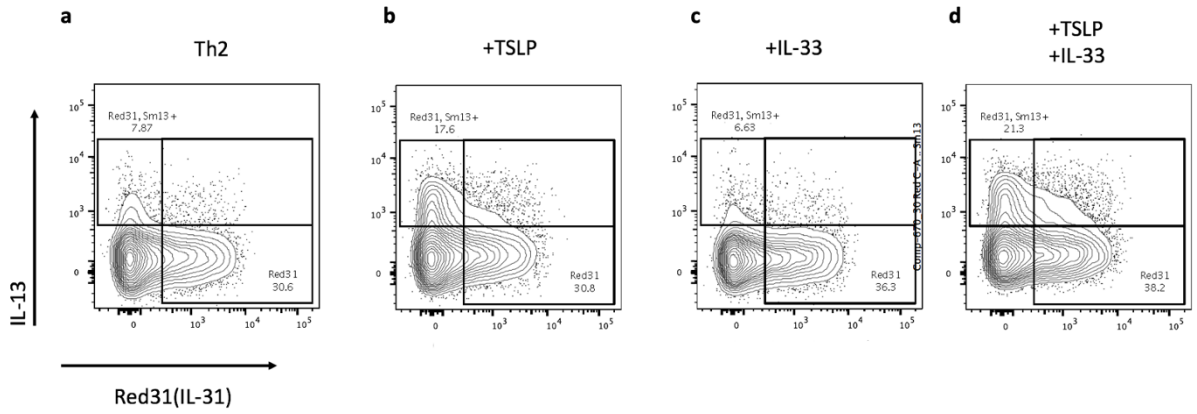

Figure 4.2 In vitro differentiated Th2 cells treated with TSLP and/or IL-33
(a,b,c,d) Representative flow plots showing Sm13 (IL-13 reporter) and R31 reporter expression in in vitro differentiated Th2 cultures a) no treatment, b) after TSLP treatment, c) after IL-33 treatment and d) after TSLP + IL-33 treatment

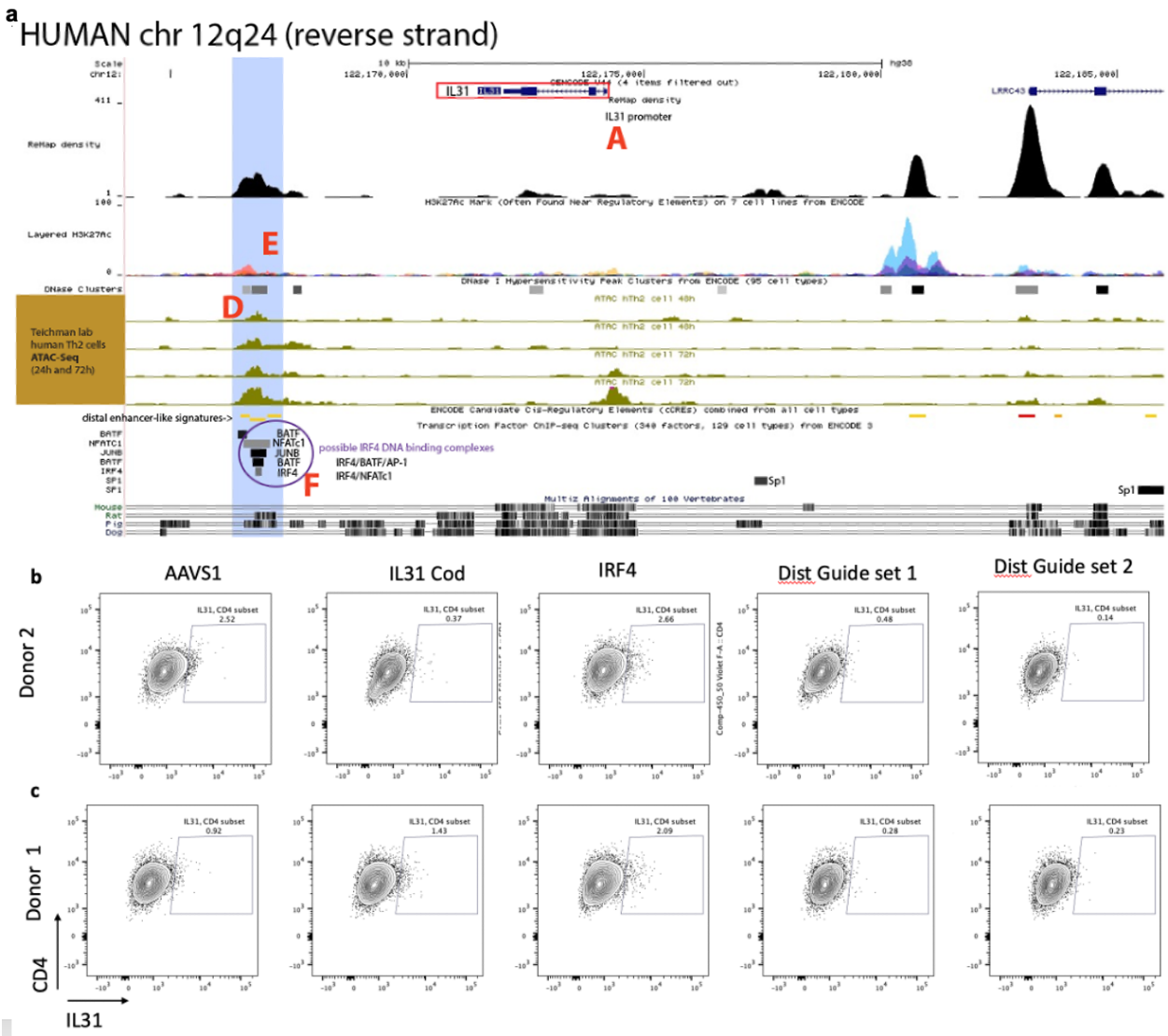

Figure 4.3 Identification of distal regulatory region of IL-31 expression
(a) genome track of *Il31* human gene showing DNAse hypersensitive site, E, ATACseq peak, D, and transcription binding sites, F (b, c) human in vitro differentiated Th2 cells targeted with crRNA via CRISPR-Cas with either AAVS1, Il31cod, Irfe, Distal Guide Set 1, or Distal guide Set 1 showing IL-31 expression

Table 4.1
Distal Regulatory sites SNP sequences

Guide 1	TCTTCATCCAAGGACCTGGA
Guide 2	TGTAAGAGCAGTGCGGTGGT
Guide 3	TGGTCAATCCATCAATCCAA
Guide 4	tctggcagattggatcagaa

Distal Regulatory sites SNP Primer Region:

tctgcatttcaCCTCCCTCTCAGCAGTACCGGCTGTGTActttgtttagaaatcactaagcatttcaagaca
gtgatgagaacagagggtgaaaacaagctcagggccctctgagctctgggccccatgactgagtaggtcacaggctcgt
gaagctggccctgCAGCCCAGAATGAAGCCTGCATGCTCTACCCAAAGGACGACGGAGC
ATTTGGTTAGCGGGTTTGCCTCTTCATCCAAGGACCTGGAAGGAGAGGAGAAATTA
GCAACTTTAAAGGTTTCCTCTCCCTGTAAGAGCAGTGCGGTGGTTTTAGTGAGAAG
AGTGCAGCGGAGTCCCCCGGCCCGTGGCTGAGTCATCTCCAGAACTGCGGGCTTT
CAGTGACAGAAGGAGAAAGGCTGAGCCTGCGCTAGATCTGCGGGAGCTCCTTGGT
CAATCCATCAATCCAATAGCATTAAATGACTCTtctggcagattggatcagaatgggaattcattaaag
gagaccaggtggttcgcagaatcgctgtgagCCTGTTGCTCATGGGAACCCGTCTGGGGTGGGG
GGCACCAGgcggccactgagagctcagcccctgttcctccagagaggggatcttgttgcaattgccacctctccgtgc
aacgaagcacctgccaccatctccgctgctttgtgtcaccagcgtctgatttgaagtctgattgcattgccg

Forward Primer:	ctgagtaggtcacaggctcg
Reverse Primer:	caattgccacctctccgtgc

REFERENCES

Ahyi, A.-N. N., Chang, H.-C., Dent, A. L., Nutt, S. L., & Kaplan, M. H. (2009). IFN regulatory factor 4 regulates the expression of a subset of Th2 cytokines. *Journal of Immunology (Baltimore, Md. : 1950)*, *183*(3), 1598–1606. https://doi.org/10.4049/JIMMUNOL.0803302

Bilsborough, J., Leung, D. Y. M., Maurer, M., Howell, M., Boguniewcz, M., Yao, L., Storey, H., LeCiel, C., Harder, B., & Gross, J. A. (2006). IL-31 is associated with cutaneous lymphocyte antigen-positive skin homing T cells in patients with atopic dermatitis. *The Journal of Allergy and Clinical Immunology*, *117*(2), 418–425. https://doi.org/10.1016/J.JACI.2005.10.046

Bilsborough, J., Mudri, S., Chadwick, E., Harder, B., & Dillon, S. R. (2010). IL-31 Receptor (IL-31RA) Knockout Mice Exhibit Elevated Responsiveness to Oncostatin M. *The Journal of Immunology*. https://doi.org/10.4049/jimmunol.0902769

Bouchery, T., Volpe, B., Shah, K., Lebon, L., Filbey, K., LeGros, G., & Harris, N. (2017). The Study of Host Immune Responses Elicited by the Model Murine Hookworms Nippostrongylus brasiliensis and Heligmosomoides polygyrus. *Current Protocols in Mouse Biology*, *7*(4), 236–286. https://doi.org/10.1002/CPMO.34

Camberis, M., Le Gros, G., & Urban, J. (2003). Animal Model of Nippostrongylus brasiliensis and Heligmosomoides polygyrus . *Current Protocols in Immunology*, *55*(1). https://doi.org/10.1002/0471142735.im1912s55

Carnevale, J., Shifrut, E., Kale, N., Nyberg, W. A., Blaeschke, F., Chen, Y. Y., Li, Z., Bapat, S. P., Diolaiti, M. E., O'Leary, P., Vedova, S., Belk, J., Daniel, B., Roth, T. L., Bachl, S., Anido, A. A., Prinzing, B., Ibañez-Vega, J., Lange, S., … Marson, A. (2022). RASA2 ablation in T cells boosts antigen sensitivity and long-term function.

Nature 2022 609:7925, *609*(7925), 174–182. https://doi.org/10.1038/s41586-022-05126-w

Cevikbas, F., & Steinhoff, M. (2012). IL-33: A novel danger signal system in atopic dermatitis. In *Journal of Investigative Dermatology*. https://doi.org/10.1038/jid.2012.66

Chang, H. Y., & Nadeau, K. C. (2017a). IL-4Rα Inhibitor for Atopic Disease. *Cell*, *170*(2), 222. https://doi.org/10.1016/J.CELL.2017.06.046

Chang, H. Y., & Nadeau, K. C. (2017b). IL-4Rα Inhibitor for Atopic Disease. *Cell*, *170*(2), 222. https://doi.org/10.1016/J.CELL.2017.06.046

Chiricozzi, A., Maurelli, M., Peris, K., & Girolomoni, G. (2020). Targeting IL-4 for the Treatment of Atopic Dermatitis. *ImmunoTargets and Therapy*, *9*, 151. https://doi.org/10.2147/ITT.S260370

Dillon, S. R., Sprecher, C., Hammond, A., Bilsborough, J., Rosenfeld-Franklin, M., Presnell, S. R., Haugen, H. S., Maurer, M., Harder, B., Johnston, J., Bort, S., Mudri, S., Kuijper, J. L., Bukowski, T., Shea, P., Dong, D. L., Dasovich, M., Grant, F. J., Lockwood, L., … Gross, J. A. (2004). Interleukin 31, a cytokine produced by activated T cells, induces dermatitis in mice. *Nature Immunology*, *5*(7), 752–760. https://doi.org/10.1038/ni1084

Doench, J. G., Fusi, N., Sullender, M., Hegde, M., Vaimberg, E. W., Donovan, K. F., Smith, I., Tothova, Z., Wilen, C., Orchard, R., Virgin, H. W., Listgarten, J., & Root, D. E. (2016). Optimized sgRNA design to maximize activity and minimize off-target effects of CRISPR-Cas9. *Nature Biotechnology 2015 34:2*, *34*(2), 184–191. https://doi.org/10.1038/nbt.3437

Fassett, M. S., Braz, J. M., Castellanos, C. A., Salvatierra, J. J., Sadeghi, M., Yu, X., Schroeder, A. W., Caston, J., Munoz-Sandoval, P., Roy, S., Lazarevsky, S., Mar, D. J., Zhou, C. J., Shin, J. S., Basbaum, A. I., & Ansel, K. M. (2023). IL-31–dependent neurogenic inflammation restrains cutaneous type 2 immune response in allergic dermatitis. *Science Immunology*, *8*(88). https://doi.org/10.1126/SCIIMMUNOL.ABI6887/SUPPL_FILE/SCIIMMUNOL.ABI6887_MDAR_REPRODUCIBILITY_CHECKLIST.PDF

Germain, R. N. (2002). T-cell development and the CD4–CD8 lineage decision. *Nature Reviews Immunology 2002 2:5*, *2*(5), 309–322. https://doi.org/10.1038/nri798

Gwack, Y., Feske, S., Srikanth, S., Hogan, P. G., & Rao, A. (2007). Signalling to transcription: Store-operated Ca2+ entry and NFAT activation in lymphocytes. *Cell Calcium*, *42*(2), 145–156. https://doi.org/10.1016/J.CECA.2007.03.007

Harvie, M., Camberis, M., Tang, S. C., Delahunt, B., Paul, W., & Le Gros, G. (2010). The Lung Is an Important Site for Priming CD4 T-Cell-Mediated Protective Immunity against Gastrointestinal Helminth Parasites. *Infection and Immunity*, *78*(9), 3753. https://doi.org/10.1128/IAI.00502-09

Hayashi, H., Kubo, Y., Izumida, M., & Matsuyama, T. (2020). Efficient viral delivery of Cas9 into human safe harbor. *Scientific Reports 2020 10:1*, *10*(1), 1–14. https://doi.org/10.1038/s41598-020-78450-8

Henriksson, J., Chen, X., Gomes, T., Ullah, U., Meyer, K. B., Miragaia, R., Duddy, G., Pramanik, J., Yusa, K., Lahesmaa, R., & Teichmann, S. A. (2019). Genome-wide CRISPR Screens in T Helper Cells Reveal Pervasive Crosstalk between Activation and Differentiation. *Cell*. https://doi.org/10.1016/j.cell.2018.11.044

Hwang, J. S., Kim, G.-C., Park, E., Kim, J.-E., Chae, C.-S., Hwang, W., Lee, C., Hwang, S.-M., Wang, H. S., Jun, C.-D., Rudra, D., & Im, S.-H. (2015). NFAT1 and JunB Cooperatively Regulate IL-31 Gene Expression in CD4 + T Cells in Health and Disease . *The Journal of Immunology*. https://doi.org/10.4049/jimmunol.1401862

Kabashima, K., Furue, M., Hanifin, J. M., Pulka, G., Wollenberg, A., Galus, R., Etoh, T., Mihara, R., Nakano, M., & Ruzicka, T. (2018). Nemolizumab in patients with moderate-to-severe atopic dermatitis: Randomized, phase II, long-term extension study. *Journal of Allergy and Clinical Immunology*. https://doi.org/10.1016/j.jaci.2018.03.018

Kabashima, K., Matsumura, T., Komazaki, H., & Kawashima, M. (2020). Trial of Nemolizumab and Topical Agents for Atopic Dermatitis with Pruritus. *New England Journal of Medicine*, *383*(2), 141–150. https://doi.org/10.1056/NEJMOA1917006/SUPPL_FILE/NEJMOA1917006_DATA-SHARING.PDF

Kishi, R., Toyama, S., Tominaga, M., Kamata, Y., Komiya, E., Kaneko, T., Suga, Y., & Takamori, K. (2023). Effects of Dupilumab on Itch-Related Events in Atopic Dermatitis: Implications for Assessing Treatment Efficacy in Clinical Practice. *Cells*, *12*(2). https://doi.org/10.3390/CELLS12020239

Klein, U., Casola, S., Cattoretti, G., Shen, Q., Lia, M., Mo, T., Ludwig, T., Rajewsky, K., & Dalla-Favera, R. (2006). Transcription factor IRF4 controls plasma cell differentiation and class-switch recombination. *Nature Immunology*, *7*(7), 773–782. https://doi.org/10.1038/NI1357

Krishnamoorthy, V., Kannanganat, S., Maienschein-Cline, M., Cook, S. L., Chen, J., Bahroos, N., Sievert, E., Corse, E., Chong, A., & Sciammas, R. (2017). The IRF4

Gene Regulatory Module Functions as a Read-Write Integrator to Dynamically Coordinate T Helper Cell Fate. *Immunity*, *47*(3), 481-497.e7. https://doi.org/10.1016/J.IMMUNI.2017.09.001/ATTACHMENT/26E3E614-0674-4310-B13E-106F8D10A233/MMC9.PDF

Kwatra, S. G., Yosipovitch, G., Legat, F. J., Reich, A., Paul, C., Simon, D., Naldi, L., Lynde, C., De Bruin-Weller, M. S., Nahm, W. K., Sauder, M., Gharib, R., Barbarot, S., Szepietowski, J. C., Conrad, C., Fleischer, A., Laquer, V. T., Misery, L., Serra-Baldrich, E., … Ständer, S. (2023). Phase 3 Trial of Nemolizumab in Patients with Prurigo Nodularis. *New England Journal of Medicine*, *389*(17), 1579–1589. https://doi.org/10.1056/NEJMOA2301333/SUPPL_FILE/NEJMOA2301333_DATA-SHARING.PDF

Lelievre, V., Favrais, G., Abad, C., Adle-Biassette, H., Lu, Y., Germano, P. M., Cheung-Lau, G., Pisegna, J. R., Gressens, P., Lawson, G., & Waschek, J. A. (2007). GASTROINTESTINAL DYSFUNCTION IN MICE WITH A TARGETED MUTATION IN THE GENE ENCODING VASOACTIVE INTESTINAL POLYPEPTIDE: A Model for the Study of Intestinal Ileus and Hirschsprung's Disease. *Peptides*, *28*(9), 1688. https://doi.org/10.1016/J.PEPTIDES.2007.05.006

Liang, H. E., Reinhardt, R. L., Bando, J. K., Sullivan, B. M., Ho, I. C., & Locksley, R. M. (2011). Divergent expression patterns of IL-4 and IL-13 define unique functions in allergic immunity. *Nature Immunology*, *13*(1), 58–66. https://doi.org/10.1038/NI.2182

Lohoff, M., Mittrücker, H. W., Prechtl, S., Bischof, S., Sommer, F., Kock, S., Ferrick, D. A., Duncan, G. S., Gessner, A., & Mak, T. W. (2002). Dysregulated T helper cell differentiation in the absence of interferon regulatory factor 4. *Proceedings of the*

National Academy of Sciences of the United States of America, *99*(18), 11808–11812. https://doi.org/10.1073/PNAS.182425099/ASSET/95A4F50C-0671-46D8-8322-C648E77EE55B/ASSETS/GRAPHIC/PQ1824250002.JPEG

Luo, C., Burgeon, E., Carew, J. A., McCaffrey, P. G., Badalian, T. M., Lane, W. S., Hogan, P. G., & Rao, A. (1996). Recombinant NFAT1 (NFATp) is regulated by calcineurin in T cells and mediates transcription of several cytokine genes. *Molecular and Cellular Biology*, *16*(7), 3955. https://doi.org/10.1128/MCB.16.7.3955

Luo, C., Shaw, K. T. Y., Raghavan, A., Aramburu, J., Garcia-Cozar, F., Perrino, B. A., Hogan, P. G., & Rao, A. (1996). Interaction of calcineurin with a domain of the transcription factor NFAT1 that controls nuclear import. *Proceedings of the National Academy of Sciences of the United States of America*, *93*(17), 8907. https://doi.org/10.1073/PNAS.93.17.8907

Lupancu, T. J., Eivazitork, M., Hamilton, J. A., Achuthan, A. A., & Lee, K. M. C. (2023). CCL17/TARC in autoimmunity and inflammation-not just a T-cell chemokine. *Immunology and Cell Biology*, *101*(7), 600–609. https://doi.org/10.1111/IMCB.12644

Madisen, L., Zwingman, T. A., Sunkin, S. M., Oh, S. W., Zariwala, H. A., Gu, H., Ng, L. L., Palmiter, R. D., Hawrylycz, M. J., Jones, A. R., Lein, E. S., & Zeng, H. (2009). A robust and high-throughput Cre reporting and characterization system for the whole mouse brain. *Nature Neuroscience 2009 13:1*, *13*(1), 133–140. https://doi.org/10.1038/nn.2467

Maier, E., Werner, D., Duschl, A., Bohle, B., & Horejs-Hoeck, J. (2014). Human Th2 but Not Th9 Cells Release IL-31 in a STAT6/NF-κB–Dependent Way. *The Journal of Immunology*. https://doi.org/10.4049/jimmunol.1301836

Maizels, R. M., & Gause, W. C. (2023). Targeting helminths: The expanding world of type 2 immune effector mechanisms. *Journal of Experimental Medicine*, *220*(10). https://doi.org/10.1084/JEM.20221381/276214

Meizoso-Huesca, A., & Launikonis, B. S. (2021). The Orai1 inhibitor BTP2 has multiple effects on Ca2+ handling in skeletal muscle. *The Journal of General Physiology*, *153*(1). https://doi.org/10.1085/JGP.202012747

Mihara, R., Kabashima, K., Furue, M., Nakano, M., & Ruzicka, T. (2019). Nemolizumab in moderate to severe atopic dermatitis: An exploratory analysis of work productivity and activity impairment in a randomized phase II study. *The Journal of Dermatology*, *46*(8), 662–671. https://doi.org/10.1111/1346-8138.14934

Mollanazar, N. K., Smith, P. K., & Yosipovitch, G. (2016). Mediators of Chronic Pruritus in Atopic Dermatitis: Getting the Itch Out? *Clinical Reviews in Allergy and Immunology*, *51*(3), 263–292. https://doi.org/10.1007/s12016-015-8488-5

Murdaca, G., Greco, M., Tonacci, A., Negrini, S., Borro, M., Puppo, F., & Gangemi, S. (2019). Il-33/il-31 axis in immune-mediated and allergic diseases. *International Journal of Molecular Sciences*, *20*(23), 1–15. https://doi.org/10.3390/ijms20235856

O'Leary, C. E., Feng, X., Cortez, V. S., Locksley, R. M., & Schneider, C. (2021). Interrogating the small intestine tuft cell – ILC2 circuit using in vivo manipulations. *Current Protocols*, *1*(3), e77. https://doi.org/10.1002/CPZ1.77

Otsuka, A., Tanioka, M., Nakagawa, Y., Honda, T., Ikoma, A., Miyachi, Y., & Kabashima, K. (2011). Effects of cyclosporine on pruritus and serum IL-31 levels in patients with atopic dermatitis. *European Journal of Dermatology : EJD*, *21*(5), 816–817. https://doi.org/10.1684/EJD.2011.1470

Park, K., Park, J.-H., Yang, W.-J., Lee, J.-J., Song, M.-J., & Kim, H.-P. (2012). Transcriptional activation of the IL31 gene by NFAT and STAT6 . *Journal of Leukocyte Biology*. https://doi.org/10.1189/jlb.0111020

Perrigoue, J. G., Li, J., Zaph, C., Goldschmidt, M., Scott, P., De Sauvage, F. J., Pearce, E. J., Ghilardi, N., & Artis, D. (2007). IL-31-IL-31R interactions negatively regulate type 2 inflammation in the lung. *Journal of Experimental Medicine*. https://doi.org/10.1084/jem.20061791

Perrigoue, J. G., Zaph, C., Guild, K., Du, Y., & Artis, D. (2009). IL-31-IL-31R Interactions Limit the Magnitude of Th2 Cytokine-Dependent Immunity and Inflammation following Intestinal Helminth Infection. *The Journal of Immunology*. https://doi.org/10.4049/jimmunol.0802459

Platt, R. J., Chen, S., Zhou, Y., Yim, M. J., Swiech, L., Kempton, H. R., Dahlman, J. E., Parnas, O., Eisenhaure, T. M., Jovanovic, M., Graham, D. B., Jhunjhunwala, S., Heidenreich, M., Xavier, R. J., Langer, R., Anderson, D. G., Hacohen, N., Regev, A., Feng, G., … Zhang, F. (2014). CRISPR-Cas9 Knockin Mice for Genome Editing and Cancer Modeling. *Cell*, *159*(2), 440. https://doi.org/10.1016/J.CELL.2014.09.014

Randak, C., Brabletz, T., Hergenröther, M., Sobotta, I., & Serfling, E. (1990). Cyclosporin A suppresses the expression of the interleukin 2 gene by inhibiting the binding of lymphocyte-specific factors to the IL-2 enhancer. *The EMBO Journal*, *9*(8), 2529. https://doi.org/10.1002/J.1460-2075.1990.TB07433.X

Ruzicka, T., Hanifin, J. M., Furue, M., Pulka, G., Mlynarczyk, I., Wollenberg, A., Galus, R., Etoh, T., Mihara, R., Yoshida, H., Stewart, J., & Kabashima, K. (2017). Anti–

Interleukin-31 Receptor A Antibody for Atopic Dermatitis. *New England Journal of Medicine*, *376*(9), 826–835. https://doi.org/10.1056/NEJMoa1606490

Saito, S., Aoki, A., Arai, I., Takaishi, S., Ito, H., Akiyama, N., & Kiyonari, H. (2017). Regulation of Th2 responses by different cell types expressing the interleukin-31 receptor. *Allergy, Asthma and Clinical Immunology*. https://doi.org/10.1186/s13223-017-0194-9

Seidl, A., Panzer, M., & Voehringer, D. (2011). Protective immunity against the gastrointestinal nematode Nippostrongylus brasiliensis requires a broad T-cell receptor repertoire. *Immunology*, *134*(2), 214. https://doi.org/10.1111/J.1365-2567.2011.03480.X

Serafini, A. T., Lewis, R. S., Clipstone, N. A., Bram, R. J., Fanger, C., Flering, S., Herzenberg, L. A., & Crabtree, G. R. (1995). Isolation of mutant T lymphocytes with defects in capacitative calcium entry. *Immunity*, *3*(2), 239–250. https://doi.org/10.1016/1074-7613(95)90093-4

Silverberg, J. I., Pinter, A., Alavi, A., Lynde, C., Bouaziz, J. D., Wollenberg, A., Murrell, D. F., Alpizar, S., Laquer, V., Chaouche, K., Ahmad, F., Armstrong, J. M., & Piketty, C. (2021). Nemolizumab is associated with a rapid improvement in atopic dermatitis signs and symptoms: subpopulation (EASI ≥ 16) analysis of randomized phase 2B study. *Journal of the European Academy of Dermatology and Venereology : JEADV*, *35*(7), 1562–1568. https://doi.org/10.1111/JDV.17218

Silverberg, J. I., Pinter, A., Pulka, G., Poulin, Y., Bouaziz, J. D., Wollenberg, A., Murrell, D. F., Alexis, A., Lindsey, L., Ahmad, F., Piketty, C., & Clucas, A. (2020). Phase 2B randomized study of nemolizumab in adults with moderate-to-severe atopic

dermatitis and severe pruritus. *Journal of Allergy and Clinical Immunology*, *145*(1), 173–182. https://doi.org/10.1016/J.JACI.2019.08.013

Sofen, H., Bissonnette, R., Yosipovitch, G., Silverberg, J. I., Tyring, S., Loo, W. J., Zook, M., Lee, M., Zou, L., Jiang, G. L., & Paolini, J. F. (2023). Efficacy and safety of vixarelimab, a human monoclonal oncostatin M receptor β antibody, in moderate-to-severe prurigo nodularis: a randomised, double-blind, placebo-controlled, phase 2a study. *EClinicalMedicine*, *57*. https://doi.org/10.1016/j.eclinm.2023.101826

Sonkoly, E., Muller, A., Lauerma, A. I., Pivarcsi, A., Soto, H., Kemeny, L., Alenius, H., Dieu-Nosjean, M. C., Meller, S., Rieker, J., Steinhoff, M., Hoffmann, T. K., Ruzicka, T., Zlotnik, A., & Homey, B. (2006). IL-31: A new link between T cells and pruritus in atopic skin inflammation. *Journal of Allergy and Clinical Immunology*. https://doi.org/10.1016/j.jaci.2005.10.033

Srikanth, S., Gwack, Y., Gwack, Y., & Srikanth, S. (2012). Orai1, STIM1, and their associating partners. *The Journal of Physiology*, *590*(17), 4169–4177. https://doi.org/10.1113/JPHYSIOL.2012.231522

Ständer, S., Yosipovitch, G., Legat, F. J., Lacour, J.-P., Paul, C., Narbutt, J., Bieber, T., Misery, L., Wollenberg, A., Reich, A., Ahmad, F., & Piketty, C. (2020). Trial of Nemolizumab in Moderate-to-Severe Prurigo Nodularis. *New England Journal of Medicine*, *382*(8), 706–716. https://doi.org/10.1056/NEJMOA1908316/SUPPL_FILE/NEJMOA1908316_DATA-SHARING.PDF

Stott, B., Lavender, P., Lehmann, S., Pennino, D., Durham, S., & Schmidt-Weber, C. B. (2013). Human IL-31 is induced by IL-4 and promotes TH2-driven inflammation.

Journal of Allergy and Clinical Immunology, *132*(2), 446-454.e5. https://doi.org/10.1016/j.jaci.2013.03.050

Vaeth, M., Kahlfuss, S., & Feske, S. (2020). CRAC Channels and Calcium Signaling in T Cell-Mediated Immunity. *Trends in Immunology*, *41*(10), 878–901. https://doi.org/10.1016/J.IT.2020.06.012

Walker, J. A., & McKenzie, A. N. J. (2017). TH2 cell development and function. *Nature Reviews Immunology 2017 18:2*, *18*(2), 121–133. https://doi.org/10.1038/nri.2017.118

Yamamura, K., Uruno, T., Shiraishi, A., Tanaka, Y., Ushijima, M., Nakahara, T., Watanabe, M., Kido-Nakahara, M., Tsuge, I., Furue, M., & Fukui, Y. (2017). The transcription factor EPAS1 links DOCK8 deficiency to atopic skin inflammation via IL-31 induction. *Nature Communications 2017 8:1*, *8*(1), 1–13. https://doi.org/10.1038/ncomms13946

Zhang, S. L., Yu, Y., Roos, J., Kozak, J. A., Deerinck, T. J., Ellisman, M. H., Stauderman, K. A., & Cahalan, M. D. (2005). STIM1 is a Ca2+ sensor that activates CRAC channels and migrates from the Ca2+ store to the plasma membrane. *Nature*, *437*(7060), 902–905. https://doi.org/10.1038/nature04147

Publishing Agreement

It is the policy of the University to encourage open access and broad distribution of all theses, dissertations, and manuscripts. The Graduate Division will facilitate the distribution of UCSF theses, dissertations, and manuscripts to the UCSF Library for open access and distribution. UCSF will make such theses, dissertations, and manuscripts accessible to the public and will take reasonable steps to preserve these works in perpetuity.

I hereby grant the non-exclusive, perpetual right to The Regents of the University of California to reproduce, publicly display, distribute, preserve, and publish copies of my thesis, dissertation, or manuscript in any form or media, now existing or later derived, including access online for teaching, research, and public service purposes.

DocuSigned by:
D468968A2214479...
Author Signature

8/2/2024
Date